

1 **Global scale evaluation of precipitation datasets for**
2 **hydrological modelling**

3 Solomon H. Gebrechorkos^{1,2}, Julian Leyland², Simon J. Dadson¹, Sagy Cohen³, Louise Slater¹,
4 Michel Wortmann¹, Philip J. Ashworth⁴, Georgina L. Bennett⁵, Richard Boothroyd⁶, Hannah
5 Cloke^{7,8}, Pauline Delorme⁹, Helen Griffith⁷, Richard Hardy¹⁰, Laurence Hawker¹¹, Stuart
6 McLelland⁹, Jeffrey Neal¹¹, Andrew Nicholas⁵, Andrew J. Tatem², Ellie Vahidi⁵, Yinxue Liu¹,
7 Justin Sheffield², Daniel R. Parsons¹⁰, Stephen E. Darby²

8 ¹School of Geography and the Environment, University of Oxford, Oxford, UK

9 ²School of Geography and Environmental Science, University of Southampton, Southampton, SO17 1BJ, United
10 Kingdom

11 ³Department of Geography and the Environment, University of Alabama, Tuscaloosa, AL, USA

12 ⁴School of Applied Sciences, University of Brighton, Sussex, BN2 4AT

13 ⁵Department of Geography, Faculty of Environment, Science and Economy, University of Exeter, Exeter, EX4
14 4RJ, United Kingdom

15 ⁶School of Geographical & Earth Sciences, University of Glasgow, UK

16 ⁷Department of Geography and Environmental Science, University of Reading, UK

17 ⁸Department of Meteorology, University of Reading, UK

18 ⁹Energy and Environment Institute, University of Hull, Hull, United Kingdom

19 ¹⁰Department of Geography, Durham University, Lower Mountjoy, South Road, Durham, DH1 3LE

20 ¹¹School of Geographical Sciences, University of Bristol, Bristol, BS8 1SS, UK

21 *Correspondence to:* Solomon H. Gebrechorkos (solomon.gebrechorkos@ouce.ox.ac.uk)

22 **Abstract.** Precipitation is the most important driver of the hydrological cycle but is challenging to estimate over
23 large scales from satellites and models. Here, we assessed the performance of six global and quasi-global high-
24 resolution precipitation datasets (European Center for Medium-range Weather Forecast (ECMWF) Reanalysis
25 version 5 (ERA5), Climate Hazards group Infrared Precipitation with Stations version 2.0 (CHIRPS), Multi-
26 Source Weighted-Ensemble Precipitation version 2.80 (MSWEP), TerraClimate (TERRA), Climate Prediction
27 Centre Unified version 1.0 (CPCU) and Precipitation Estimation from Remotely Sensed Information using
28 Artificial Neural Networks-Cloud Classification System-Climate Data Record (PERCCDR)) for hydrological
29 modelling globally and quasi-globally. We forced the WBMsed global hydrological model with the precipitation
30 datasets to simulate river discharge from 1983 to 2019 and evaluated the predicted discharge against 1825
31 hydrological stations worldwide, using a range of statistical methods. The results show large differences in the
32 accuracy of discharge predictions when using different precipitation input datasets. Based on evaluation at annual,
33 monthly and daily time scales, MSWEP followed by ERA5 demonstrated a higher correlation (CC) and Kling-
34 Gupta Efficiency (KGE) than other datasets for more than 50% of the stations. Whilst ERA5 was the second-
35 highest performing dataset and it showed the highest error and bias in about 20% of the stations. The PERCCDR
36 is the least well-performing dataset with bias of up to 99% and a normalised root mean square error of up to 247%.
37 PERCCDR only show a higher KGE and CC than the other products in less than 10% of the stations. Even though
38 MSWEP provided the highest performance overall, our analysis reveals high spatial variability, meaning that it is
39 important to consider other datasets in areas where MSWEP showed a lower performance. The results of this
40 study provide guidance on the selection of precipitation datasets for modelling river discharge for a basin, region
41 or climatic zone as there is no single best precipitation dataset globally. Finally, the large discrepancy in the
42 performance of the datasets in different parts of the world highlights the need to improve global precipitation data
43 products.

44
45
46
47
48
49
50
51
52
53
54
55
56

57 **1. Introduction**

58 Whilst precipitation is one of the most important components of the global hydrological cycle and regulates the
59 climate system (Miao et al., 2019; Sadeghi et al., 2021), it remains one of the most challenging variables to
60 estimate at a global scale using satellite data and modelling approaches (Michaelides et al., 2009; Kidd and
61 Levizzani, 2011; Beck et al., 2017a; Ursulak and Coulibaly, 2021). Reliable precipitation data with sufficient
62 spatial and temporal coverage and accurate representation of extreme events is crucial for various applications.
63 These include the development of water resource management and planning strategies, hydrological applications
64 including forecasting hydrological extremes, and climate change analysis (Mehran and AghaKouchak, 2014;
65 Nguyen et al., 2018; Sadeghi et al., 2021; Acharya et al., 2019). Observed precipitation from meteorological
66 stations is typically used at local to river basin scale with gauge-based gridded precipitation datasets, such as from
67 the Global Historical Climatology Network (Menne et al., 2012), developed to study climate and hydrology over
68 larger scales. However, precipitation from gauges and gauge-based gridded datasets have several drawbacks such
69 as limited spatial and temporal coverage, prevalence of missing values, and limited accuracy in sparsely populated
70 and remote areas (Kidd and Levizzani, 2011; Reichle et al., 2011; Kidd et al., 2017; Sun et al., 2018; Gebrechorkos
71 et al., 2018; Hafizi and Sorman, 2022). In addition, data-sharing policies have caused significant challenges in
72 obtaining data, particularly in developing countries (Gebrechorkos et al., 2018; Hafizi and Sorman, 2022).

73 Given the challenges in representing precipitation at global scales, satellite, climate model, and reanalysis-based
74 precipitation datasets can form the basis for monitoring and prediction of water resources and hydrological
75 extremes, particularly in data-scarce regions of the world (Sheffield et al., 2018; Dembélé et al., 2020).
76 Nevertheless, uncertainties and errors in these datasets require careful analysis to assess their suitability for a
77 specific use. Error in satellite-based precipitation estimates can be due to errors in the sensor measurements, the
78 frequency of sampling, and the retrieval algorithms, including the representation of cloud physics (Dembélé et al.,
79 2020; Laiti et al., 2018; Alazzy et al., 2017). Climate model-based datasets, including reanalyses, have large
80 uncertainty due to their coarse spatial resolution and ambiguity associated with model parameters (Gebrechorkos
81 et al., 2018; AL-Falahi et al., 2020; Dembélé et al., 2020; Her et al., 2019). Reanalysis datasets may correct for
82 some of these errors via the assimilation of observational data, but this comes with its own uncertainties due to
83 the error characteristics of the assimilated observations and the assimilation scheme (Sheffield et al., 2006; Parker,
84 2016). In hydrological modelling, errors and biases in precipitation data result in poor representation of the
85 hydrological responses and affect applications (Maggioni and Massari, 2018; Zambrano-Bigiarini et al., 2016).
86 For example, according to Bárdossy et al. (2022), uncertainty in precipitation can lead to hydrological model
87 errors of up to 50%. Hence, it is important to assess the quality and accuracy of the precipitation products before
88 using them in global or basin-scale hydrological models. In data-limited regions, hydrological models driven by
89 precipitation datasets developed from satellite sources, reanalysis or climate models are the only plausible way to
90 represent the terrestrial water cycle (van Huijgevoort et al., 2013).

91 Over the last few decades, several global and quasi-global precipitation datasets have been developed that address
92 some of these challenges and can be used to drive hydrological models at regional and global scales. These
93 precipitation datasets differ in terms of their spatial resolution, spatial coverage (e.g., global or regional), data
94 sources (e.g., gauge, satellite, reanalysis, and radar), temporal resolution (e.g., sub-daily and daily), and length of

95 record. It is therefore important to evaluate the accuracy of the datasets before they are used to drive global or
96 regional scale hydrological models. Most studies have evaluated precipitation datasets using observed data from
97 field-based meteorological stations at a range of scales (e.g., Beck et al., 2017a; Gebrechorkos et al., 2018; Xiang
98 et al., 2021; Sun et al., 2018; Hong et al., 2022; Wati et al., 2022; AL-Falahi et al., 2020; Ahmed et al., 2019;
99 Fallah et al., 2020). Hydrological models have also been used to assess the quality of the precipitation dataset by
100 comparing simulated and observed discharge across different spatial scales (e.g., Mazzoleni et al., 2019; Beck et
101 al., 2017a; Zhu et al., 2018; Raimonet et al., 2017; Guo et al., 2018; Wang et al., 2020; Salehi et al., 2022; Zhu et
102 al., 2018; Seyyedi et al., 2015). In principle, this latter approach is able to identify the precipitation datasets which
103 best represent hydrological variability including extremes, even in catchments where there have been multiple
104 drivers of change.

105 There are a limited number of studies assessing multiple precipitation datasets for global hydrological model
106 applications (Voisin et al., 2008; Beck et al., 2017a; Mazzoleni et al., 2019). Voisin et al. (2008) conducted a
107 global-scale evaluation of two precipitation for hydrological modelling. Beck et al., (2017a) compared the
108 performance of 22 precipitation datasets for global hydrological modelling. Mazzoleni et al. (2019) evaluated 18
109 different precipitation datasets in eight river basins on different continents. Both Beck et al. (2017a) and Mazzoleni
110 et al. (2019) found that merged satellite-observation precipitation products showed the best performance compared
111 to satellite-only products. These studies exclusively concentrate on a daily time scale, evaluating performance
112 solely through the Nash-Sutcliffe Efficiency (NSE). Neither study extends this assessment to monthly and annual
113 time scales, and notably, they do not assess the hydrological extremes which are often considered important to
114 capture. Here, we build upon the work by Beck et al., (2017a) by adding recently developed high-resolution
115 precipitation datasets. These include the European Center for Medium-range Weather Forecast (ECMWF)
116 Reanalysis version 5 (ERA5) (Hersbach et al., 2020), TerraClimate (Abatzoglou et al., 2018) and Precipitation
117 Estimation from Remotely Sensed Information using Artificial Neural Networks-Cloud Classification System-
118 Climate Data Record (PERCCDR, Sadeghi et al., 2021) and the latest Multi-Source Weighted-Ensemble
119 Precipitation version 2.80 (MSWEP). These additions significantly broaden the scope of our study, offering a
120 diverse range of products with distinct methodologies. In addition, we use multiple statistical metrics to evaluate
121 the performance of the precipitation products for hydrological modelling at daily, monthly and annual time scales
122 and for daily extremes, which represents a current gap in the modelling literature.

123 The aim of this study is to undertake a comprehensive evaluation, spanning various temporal and spatial scales,
124 to examine how different input precipitation datasets impact the predictions of a global hydrological model. We
125 assess six high-resolution precipitation datasets, each with records spanning over 30 years. A comprehensive and
126 physically based gridded global hydrological model (WBMsed; Cohen et al., (2013)) is used to simulate river
127 discharge globally. The model incorporates various datasets, including reservoirs, dams, and crop water
128 requirements, which significantly influence streamflows. The objective is not to evaluate the absolute performance
129 of the hydrological model, which can be influenced by local factors, rather our focus is on comparing the relative
130 performance of the six precipitation datasets at individual locations. The modelled discharge, derived from the six
131 precipitation datasets, is assessed across the various time scales by comparing it with observed discharge data
132 collected from 1825 river gauge stations worldwide. Furthermore, we assess the performance of the precipitation
133 products by examining their accuracy in representing daily extreme precipitation events across various percentiles.

134 In summary, this research offers a thorough evaluation of this set of diverse precipitation products, spanning from
135 daily extreme events to annual time scales, providing an invaluable resource for selecting appropriate basin-to-
136 regional-to-global scale inputs for hydrological modelling applications.

137 **2. Data and methods**

138 In the following sections, we outline the various input and evaluation datasets which were used within the
139 WBMsed hydrological modelling framework. The statistical evaluation methods used to assess the results are also
140 outlined.

141 **2.1. Precipitation datasets**

142 The precipitation datasets used herein are selected based on their length of record (>30 years period), spatial
143 coverage (global and quasi-global) and recommendations from previous research (Beck et al., 2017a) (Table 1).
144 Based on the findings of Beck et al. (2017a), datasets with low performance were excluded, while those
145 demonstrating the highest performance, such as MSWEP and Climate Hazards group Infrared Precipitation with
146 Stations version 2.0 (CHIRPS), were retained, and new datasets were incorporated. The selected precipitation
147 datasets are the ERA5 ERA5, CHIRPS, MSWEP, TerraClimate (TERRA), Climate Prediction Centre Unified
148 version 1.0 (CPCU), and PERCCDR. Due to their spatial coverage, CHIRPS and PERCCDR are evaluated only
149 up to latitudes of 50°N and 60°N, respectively (Table 1). Each dataset was subsequently used to force the WBMsed
150 hydrological model, to generate streamflow estimates. The availability of these datasets with longer records
151 enables the assessment of long-term hydrological changes at global, regional, and catchment scales.

152 ERA5 is the fifth generation European Centre for Medium-Range Weather Forecasts (ECMWF) reanalysis data
153 available globally from 1940 to present (Hersbach et al., 2020). ERA5 combines modelled data and observations
154 to create a complete and consistent global climate dataset using advanced data assimilation methods. ERA5
155 provides improved precipitation representation such as the inclusion of tropical cyclones when compared to the
156 ERA-Interim (He et al., 2020; Jiao et al., 2021). In addition, ERA5-Land, a subset of ERA5 focusing on land
157 areas, delivers more detailed climate information at higher spatial resolution (0.1°) from 1950 to the present
158 compared to ERA5 (Hersbach et al., 2020). Here, ERA5-Land (referred to as ERA5) is used to evaluate its
159 performance for global hydrological modelling. The data is freely available from Copernicus Climate Data Store
160 (<https://cds.climate.copernicus.eu/cdsapp#!/dataset/reanalysis-era5-land?tab=overview>).

161 CHIRPS is a high-resolution (0.05°) quasi-global rainfall product primarily developed for monitoring droughts
162 and global environmental changes (Funk et al., 2015). CHIRPS provides coupled gauge-satellite precipitation
163 estimates with a 0.05° spatial resolution and long-period records. The product is developed by combining satellite-
164 only Climate Hazards group Infrared Precipitation (CHIRP), Climate Hazards group Precipitation climatology
165 (CHPclim), and data from ground stations. CHIRP and CHPclim were developed based on calibrated infrared
166 cold cloud duration (CCD) precipitation estimates and ground station data from the Global Historical Climate
167 Network (GHCN). The product is available at the Climate Hazards Group (<https://www.chc.ucsb.edu/data/chirps/>)
168 on daily, 10-day, and monthly timescales from the 1981-near present. Due to its availability at high spatial and
169 temporal resolution, CHIRPS is widely used in hydrological studies (Luo et al., 2019; Gebrechorkos et al., 2020;

170 Geleta and Deressa, 2021; Wang et al., 2021; Opere et al., 2022; Day and Howarth, 2019; Gebrechorkos et al.,
171 2019) and modelling of hydrological extremes such as droughts and floods (Chen et al., 2020; Mianabadi et al.,
172 2022; Peng et al., 2020).

173 MSWEP is a global high-resolution (0.1°) precipitation product developed by merging multiple datasets such as
174 ground stations (~77,000), satellite-based rainfall estimates, and reanalysis data (Beck et al., 2019b). MSWEP
175 was developed by merging station data satellite datasets and reanalysis datasets (Beck et al., 2017b, 2019b).
176 MSWEP has been widely used in regional and global scale hydrological studies such as for floods and droughts
177 (Gu et al., 2023; Gebrechorkos et al., 2022b; Reis et al., 2022; Wu et al., 2018; Sun et al., 2022; Gebrechorkos et
178 al., 2022c; Xiang et al., 2021; López López et al., 2017) and for developing high-resolution global scale
179 hydrological extreme and climate datasets and regional drought monitoring (Gebrechorkos et al., 2023, 2022a; Li
180 et al., 2022b). MSWEP is available from 1979-present at multiple timescales (e.g., 3 hourly) and can be accessed
181 from the GloH2O website (<https://www.gloh2o.org/mswep/>).

182 TerraClimate (TERRA) is a high-resolution (0.04°) terrestrial monthly climate (e.g., precipitation and
183 temperature) and climatic water-balance dataset available from 1958-2020 (Abatzoglou et al., 2018). TERRA was
184 developed by combining high and coarse spatial resolution datasets such as WorldClim climatological normals
185 and Climatic Research Unit gridded Time Series (CRU TS) and JRA-55, respectively. The data was evaluated
186 against ground observation from the Historical Climate Network and exhibited better performance than the CRU-
187 TS (Abatzoglou et al., 2018). The monthly climate and climatic water balance is available from the Climatology
188 Lab website (<https://www.climatologylab.org/>).

189 CPCU is a gauge-based analysis of daily precipitation datasets available globally from 1979 to present at a spatial
190 resolution of 0.5° (Chen et al., 2008). CPCU is the product of the CPC Unified Precipitation project at NOAA
191 Climate Prediction Center. The product uses data from more than 30,000 (1979-2005) and 17,000 (2006-present)
192 stations. The CPCU data is publicly available at the NOAA Physical Sciences Laboratory (PSL,
193 https://downloads.psl.noaa.gov/Datasets/cpc_global_precip/) and has been used for hydrological and climate
194 studies (Beck et al., 2017a; Zhu et al., 2021; Hou et al., 2014).

195 The PERCCDR is a quasi-global (latitude from 60°S to 60°N) dataset developed at the University of California
196 (Sadeghi et al., 2021). PERCCDR provides precipitation estimates at high spatial (0.04°) and temporal (3-hourly)
197 resolutions from 1983 to present. The dataset is developed using the rain rate output from the PERSIANN-CCS
198 model, which uses GridSat-B1 IR and NOAA Climate Prediction Center (CPC-4km) IR data. Compared to other
199 PERSIANN precipitation datasets, PERCCDR provides a realistic representation of precipitation extremes
200 globally and shows better agreement with CPCU precipitation (Sadeghi et al., 2021). The PERCCDR has been
201 used in hydrological studies (Salehi et al., 2022; Eini et al., 2022) and is freely available from the Center for
202 Hydrometeorology and Remote Sensing (CHRS) Data Portal (<https://chrsdata.eng.uci.edu/>).

203 Table 1. The six precipitation datasets used in this study, their spatial and temporal resolution, spatial coverage
204 and data sources.

Abbreviation	Full name	Spatial resolution and coverage	Temporal resolution	Temporal coverage	Data source	Reference
ERA5	ECMWF (European Centre for Medium-Range Weather Forecasts) Reanalysis V5	0.1°, global	Sub-daily	1979-present	Gauge and reanalysis	(Hersbach et al., 2020)
CHIRPS	Climate Hazards group Infrared Precipitation with Stations (CHIRPS) version 2.0	0.05°, quasi global (50°S-50°N)	Daily	1981-present	Gauge, satellite, and reanalysis	(Funk et al., 2015)
MSWEP	Multi-Source Weighted-Ensemble Precipitation (MSWEP) version 2.80	0.1°, global	Daily	1979-present	Gauge, satellite, and reanalysis	(Beck et al., 2019b)
TERRA	TerraClimate	0.042°, global	Monthly	1958-present	Gauge and reanalysis	(Abatzoglou et al., 2018)
CPCU	Climate Prediction Centre (CPC) Unified V1.0	0.5°, global	Daily	1979-present	Gauge only	(Chen et al., 2008)
PERCCDR	Precipitation Estimation from Remotely Sensed Information using Artificial Neural Networks-Cloud Classification System-Climate Data Record (PERSIANN-CCS-CDR)	0.04°, Quasi global (60°S-60°N)	Sub-daily	1983-present	Gauge and satellite	(Sadeghi et al., 2021)

205 2.2. WBMsed hydrological model

206 The WBMsed (Cohen et al., 2013, 2014) model is used to assess the performance of the different precipitation
207 datasets for hydrological modelling globally. WBMsed is a global-scale hydrogeomorphic model, an extension of
208 the WBMplus global hydrology model (Wisser et al., 2010), which is part of the FrAMES biogeochemical
209 modelling framework (Wollheim et al., 2008). The WBMplus model is one of the first Global Hydrological
210 Models (GHMs) applied to a global domain (Cohen et al., 2013; Grogan et al., 2022). The WBMsed model extends
211 the WBMplus model by including sediment flux modules (suspended, bedload and suspended bed material; Cohen

212 et al. 2022). While we are not analyzing sediment flux in this paper, we opted to use the WBMsed model for
213 consistency with consequent analysis. The hydrological prediction of WBMsed is equivalent to WBMplus.

214 The model represents the major hydrological cycle components of the land surface and tracks the balances and
215 fluxes between the atmosphere, surface water storages, vegetation, runoff, and groundwater (Grogan et al., 2022).
216 The model includes hydrological infrastructure (e.g., dams and reservoirs), agricultural water requirements, and
217 domestic and industrial water uses. A gridded river network connects grid cells, which allows the routing of fluxes
218 downstream (e.g., streamflow). The model requires several climate datasets as input in addition to precipitation,
219 including temperature, humidity, air pressure, and wind speed (Table S1). Additional parameters such as field
220 capacity, rooting depth, and riverbed slope are used to drive the model.

221 We use an identical model setup to that used by Cohen et al., (2022) with all input datasets as detailed in Cohen
222 et al. (2013). Updates include daily ERA5 air temperature (Hersbach et al., 2020) re-gridded at 10 arc-minutes
223 resolution, reservoir capacity from the global reservoir and dam database (GRanD v1.3; Lehner et al., (2011)),
224 and a 6 arc-minute HydroSTN30 network derived from HydroSHEDS (Lehner et al., 2008). In addition, we used
225 each of the six input precipitation datasets, ERA5, CHIRPS, MSWEP, TERRA, CPCU, and PERCCDR in turn,
226 keeping all other parameters and inputs the same. All the input precipitation datasets are bilinearly interpolated to
227 the same spatial resolution of 0.1°. Even though WBMsed can disaggregate monthly time series into daily,
228 TERRA (only available at monthly resolution, see Table 1) is evaluated on monthly and annual time scales, whilst
229 all other datasets are evaluated at daily, monthly and annual time scales. WBMsed simulations were run at 0.1°
230 (~11km at the equator) spatial and daily and monthly temporal resolutions. Several WBMsed streamflow
231 validation analyses have been reported previously (e.g., Cohen et al., 2022; Dunn et al., 2019; Cohen et al., 2014,
232 2013; Moragoda and Cohen, 2020), which indicate that the model represents the long-term average observed
233 streamflow globally. It is important to note that this study assesses the precipitation datasets without calibration
234 of the WBMsed model for each precipitation dataset, which could theoretically improve their performance in
235 replicating observed river discharge.

236 **2.3. Observed river discharge from ground stations**

237 Observed daily and monthly river discharge used to evaluate the hydrological model were obtained from the
238 Global Runoff Data Centre (GRDC, 2023). The GRDC is an international data archive
239 (<https://www.bafg.de/GRDC/>), which hosts data for over 10,000 hydrological stations. The number of stations
240 with a length of record greater than 10 years during the evaluation period (1981-2019) are limited. Here, we
241 consider stations with a minimum record length of 10 years, allowing for missing values within this period. Due
242 to the spatial resolution of the input datasets and the model simulations (~11x11 km), we only consider stations
243 with a catchment area of greater than 100 km². Overall, 1825 suitable stations were identified with daily and
244 monthly records, largely in North and South America, Europe and Australia, with very few stations in Africa and
245 Asia (Figure 1).

246 **2.4. Evaluation metrics**

247 Several methods are used to assess the modelled discharge using the streamflow observations: the Pearson
 248 correlation coefficient (CC, Eq. 1), Kling-Gupta Efficiency (KGE, Eq. 2) (Gupta et al., 2009), Root-Mean-Square
 249 Error (RMSE, Eq.3) and Percentage of bias (Pbias, Eq.4). CC measures the linear relationship between observed
 250 discharge and simulated discharge, focusing primarily on the degree of association between the two datasets. It is
 251 particularly useful for assessing the strength and direction of this relationship, highlighting how well the model
 252 captures the variability in discharge (Moazami et al., 2013). KGE is a comprehensive metric that evaluates the
 253 overall agreement between observed and simulated streamflow, considering similarities in variability, amplitude,
 254 and timing. It provides an assessment of the model's ability to capture both the magnitude and temporal dynamics
 255 of the observed discharge (Gupta et al., 2009). RMSE measures the average magnitude of the differences between
 256 observed and simulated discharge, providing a measure of the overall goodness of fit. Moreover, the percentage
 257 of bias is used to quantify the systematic overestimation or underestimation of discharge by the model compared
 258 to observations (Moazami et al., 2013). A KGE value of 1.0 indicates a perfect match between the observed and
 259 simulated discharge, whereas values lower than -0.41 show that the model is worse than using the mean of the
 260 observed discharge as a predictor (Knoben et al., 2019). For spatial comparison, the RMSE is normalised by the
 261 standard deviation of the observed data (NRMSE; Eq. 5).

262
$$CC = \frac{\sum_{i=1}^N (M_i - \bar{M}) * (O_i - \bar{O})}{\sqrt{\sum_{i=1}^N (M_i - \bar{M})^2} * \sqrt{\sum_{i=1}^N (O_i - \bar{O})^2}} \quad (1)$$

263
$$KGE = 1 - \sqrt{(r - 1)^2 + (\alpha - 1)^2 + (\beta - 1)^2} \quad (2)$$

264
$$RMSE = \sqrt{\frac{\sum_{i=1}^N (O_i - M_i)^2}{N}} \quad (3)$$

265
$$Pbias = \frac{\sum_{i=1}^N (M_i - O_i)}{\sum_{i=1}^N O_i} * 100 \quad (4)$$

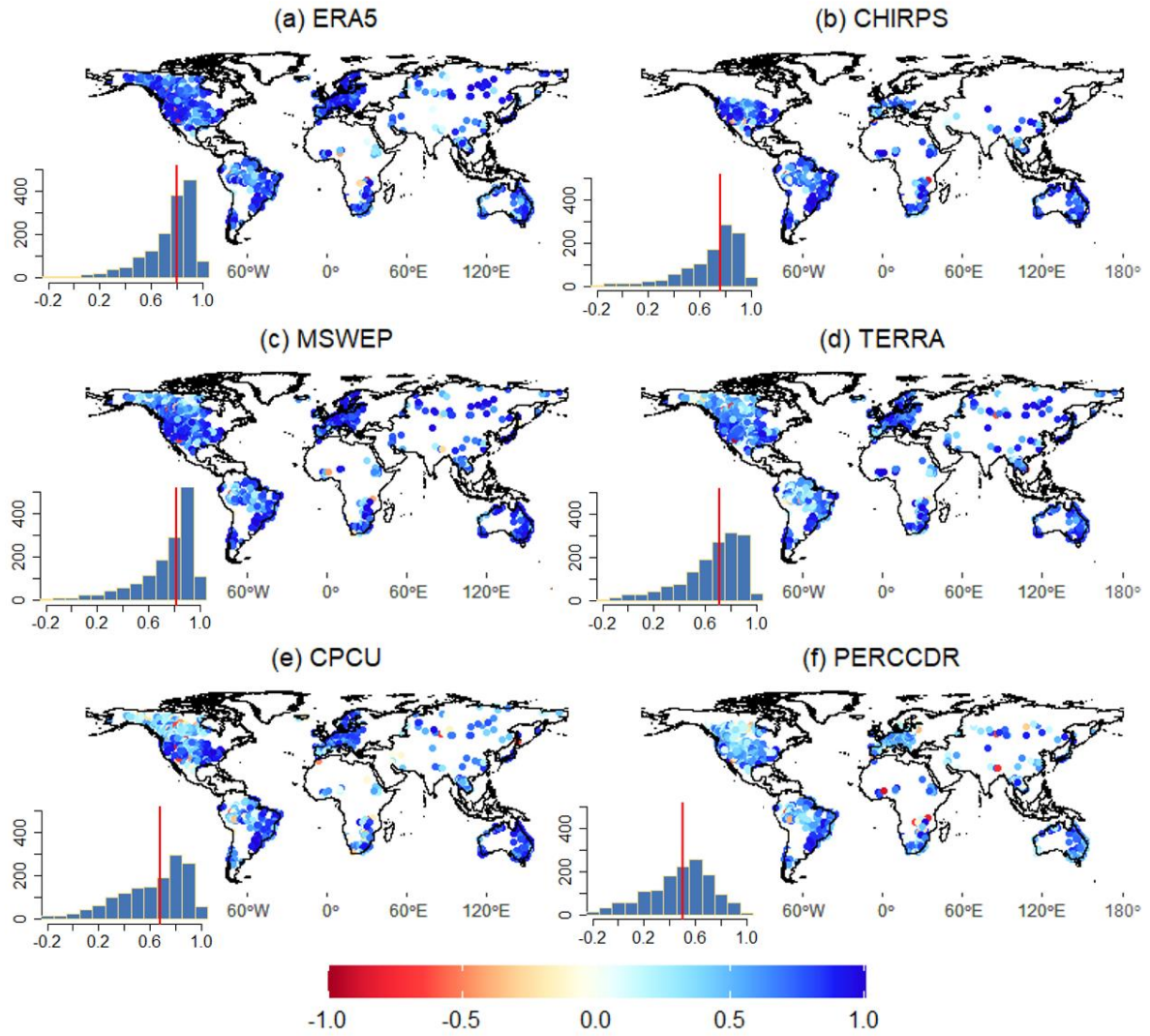
266
$$NRMSE = \frac{RMSE}{SD} * 100 \quad (5)$$

267 where r is the linear correlation between observed (O) and modelled (M) discharge and α and β are the variability
 268 and bias ratios, respectively. The NRMSE and SD are the normalised RMSE and standard deviation, respectively.
 269 To assess the performance of the precipitation datasets for representing daily hydrological extremes, the 90th and
 270 10th percentile are used, which indicates high and low flows, respectively. To derive high and low flow thresholds
 271 from a daily flow time series, the data is first arranged in ascending order. The 90th percentile (Q10) is then
 272 determined as the flow value above which 90% of the daily flows lie, representing high-flow conditions. Similarly,
 273 the 10th percentile (Q90) represents the flow value below which 90% of the daily flows occur, indicating low-flow
 274 conditions.

275 **3. Results**

276 **3.1. Performance of the six precipitation datasets for annual discharge prediction**

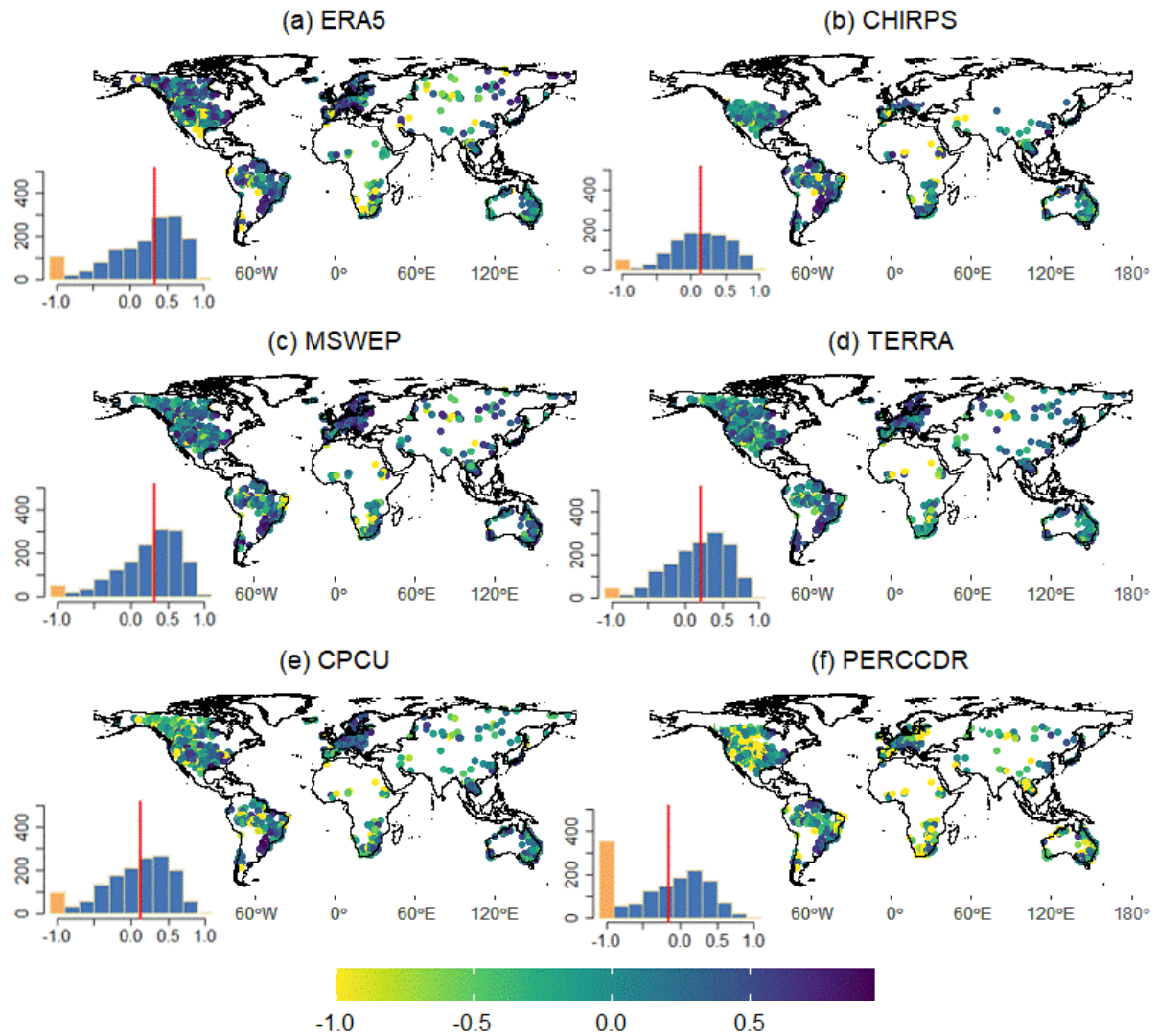
277 The temporal correlation coefficient (CC) between the observed and simulated annual discharge based on the six
278 precipitation datasets is summarised in Figure 1. Most of the datasets, particularly ERA5, MSWEP, and CHIRPS,
279 showed a high CC in basins of Europe (e.g., Danube basin), South America (e.g., Rio de la Plata-Parana), North
280 America and Australia (e.g., Murray-Darling). MSWEP and ERA5 showed the highest CC for 34% and 32% of
281 the stations, respectively, followed by CPCU and CHIRPS. The TERRA and PERCCDR were the least well-
282 performing datasets with lower CC overall, and a higher CC than other datasets for less than 9% of stations. The
283 median CC of MSWEP and ERA5 is 0.82 and 0.8, respectively. MSWEP and TERRA showed lower Pbias and
284 NRMSE compared to the other datasets (Figures S1 and S2). ERA5 and PERCCDR showed a high NRMSE (up
285 to 247%) and Pbias (up to 99%) for more than 46% of stations. Similar to the CC, ERA5 and MSWEP
286 outperformed the other datasets for KGE, with higher values for 32% and 27% of stations, respectively. The
287 performance of MSWEP and ERA5 is higher in basins of Europe, South America, and Australia compared to Asia
288 and Africa. The median KGE values of ERA5 and MSWEP are 0.33 and 0.32, respectively (Figure 2). The
289 PERCCDR and CPU demonstrate high KGE only in about 9% of the stations, with median values of 0.10 and
290 0.13, respectively. Based on the annual CC and KGE, there is no single precipitation dataset that is best
291 everywhere, and even the least well-performing dataset overall shows better performance in some stations (Figure
292 3). Figure 3 summarizes the spatial representation of precipitation dataset performance, highlighting the individual
293 datasets exhibiting the highest CC and KGE values at each observation point.



294

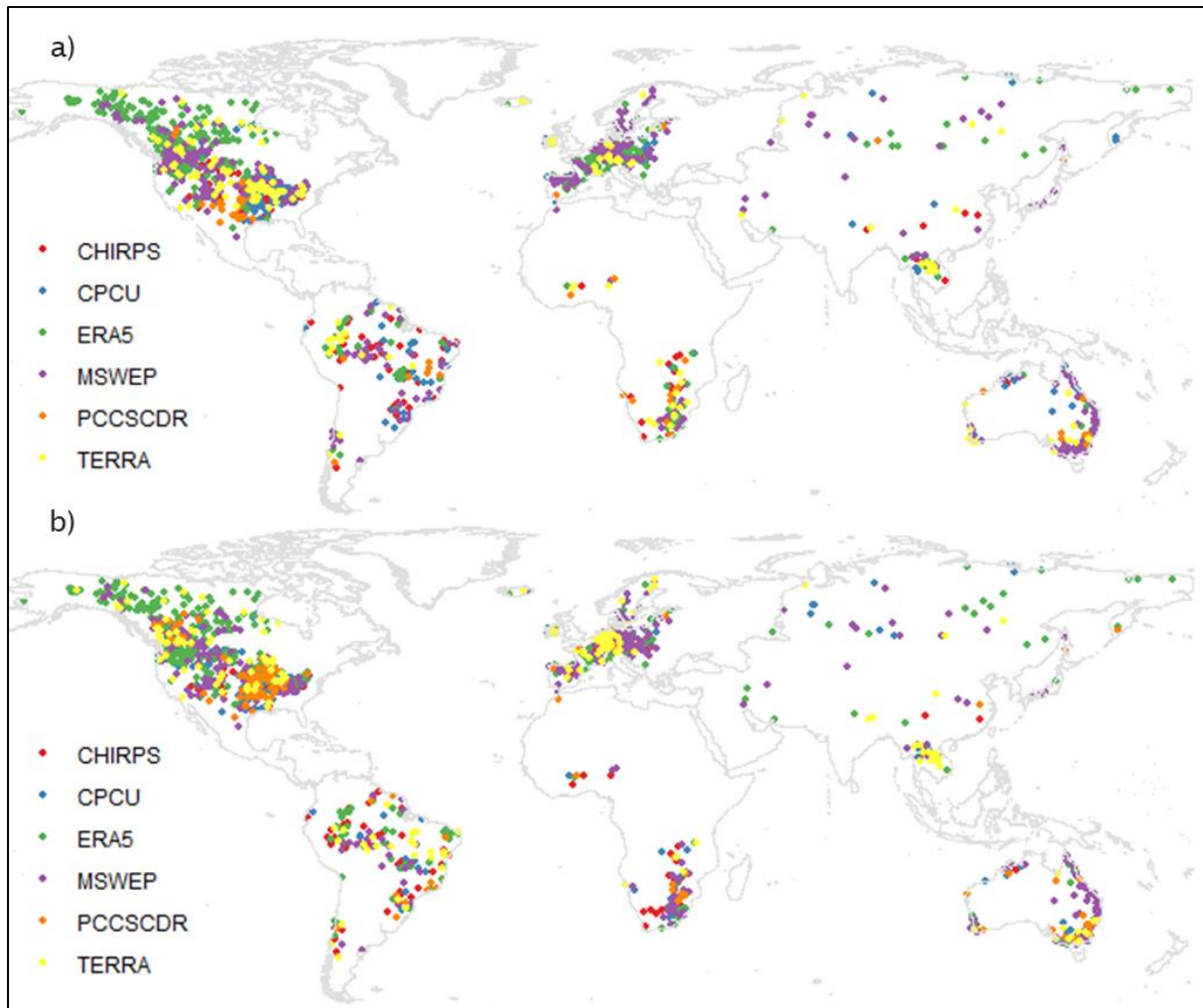
295 **Figure 1: Correlation (CC) between annual observed and modelled streamflow data using a) ERA5, b) CHIRPS, c)**
 296 **MSWEP, d) TERRA, e) CPCU and f) PERCCDR precipitation datasets. The inset histograms show the frequency**
 297 **distribution (y-axis) of the annual CC (x-axis), with the red vertical line indicating the median value.**

298



299

300 Figure 2: KGE between observed and modelled annual streamflow based on a) ERA5, b) CHIRPS, c) MSWEP, d)
 301 TERRA, e) CPCU, and f) PERCCDR precipitation datasets. KGE values below -0.41 indicate bad model performance
 302 than using observed discharge mean as a predictor. The inset histograms show the frequency distribution (y-axis) of
 303 the annual KGE (x-axis). KGE values lower than -1 are highlighted in orange. The red vertical line indicates the median
 304 value.

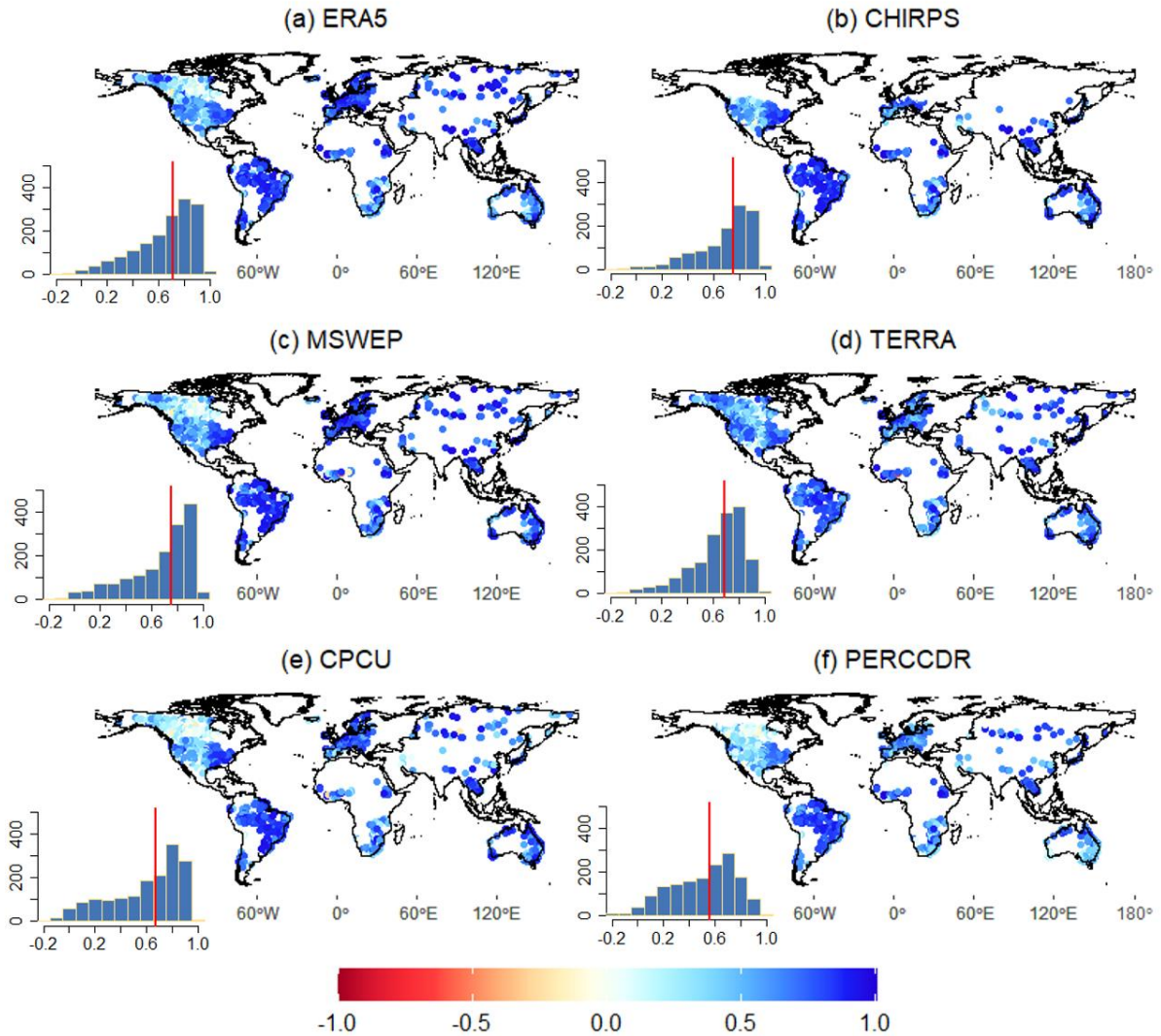


305

306 **Figure 3: The best performing precipitation dataset (ERA5, CHIRPS, MSWEP, TERRA, CPCU, and PERCCDR) at**
 307 **each of the observed discharge stations based on annual CC (a) and KGE (b).**

308 **3.2. Performance of the six precipitation datasets for monthly discharge predictions**

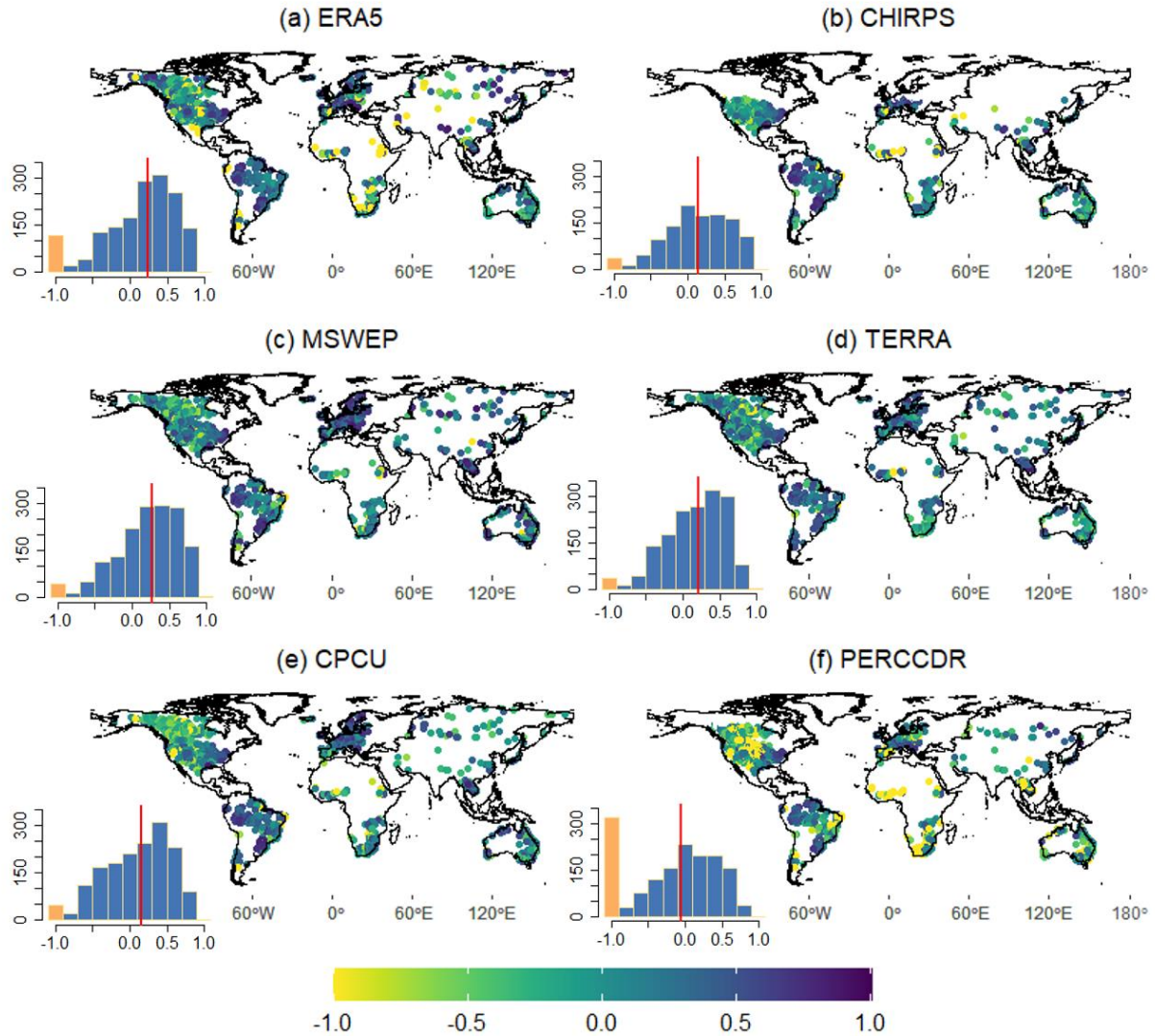
309 The six precipitation datasets consistently demonstrate high CC at a monthly scale in large parts of the world,
 310 except in some rivers of Canada and Australia (Figure 4). The monthly CC, similar to the annual CC, shows a
 311 relatively better performance of MSWEP with a median CC of 0.76. TERRA is the second-best with a median
 312 CC of 0.69. MSWEP and TERRA show a higher CC than other datasets in 35% and 28% of the stations,
 313 respectively. ERA5 and CHIRPS are ranked as the third and fourth datasets with a median CC of 0.71 and 0.75,
 314 respectively. CPCU and PERCCDR are the least well-performing datasets, which only show the highest CC in
 315 less than 6% of the stations with a median CC of 0.67 and 0.56, respectively.



316

317 **Figure 4: Correlation (CC) between monthly observed and modelled streamflow data based on a) ERA5, b) CHIRPS,**
 318 **c) MSWEP, d) TERRA, e) CPCU and f) PERCCDR precipitation datasets. The inset histograms show the frequency**
 319 **distribution (y-axis) of the monthly CC (x-axis), with the red vertical line indicating the median value.**

320 The monthly KGE also indicates the better performance of ERA5 and MSWEP for 26% and 24% of stations,
 321 respectively (Figure 5). MSWEP showed a lower Pbias and NRMSE than all datasets, except in 5% of the stations
 322 (Figures S3 and S4). Compared to MSWEP, ERA5 showed a larger Pbias and NRMSE in 15% and 19% of the
 323 stations. TERRA, a third-best performing dataset based on KGE (18% of stations), shows a lower monthly Pbias
 324 and RMSE in 85% of the stations compared to CHIRPS, ERA5, and PERCCDR. Compared to all datasets, the
 325 PERCCDR showed a higher NRMSE and Pbias in 55% and 28% of the stations, respectively.

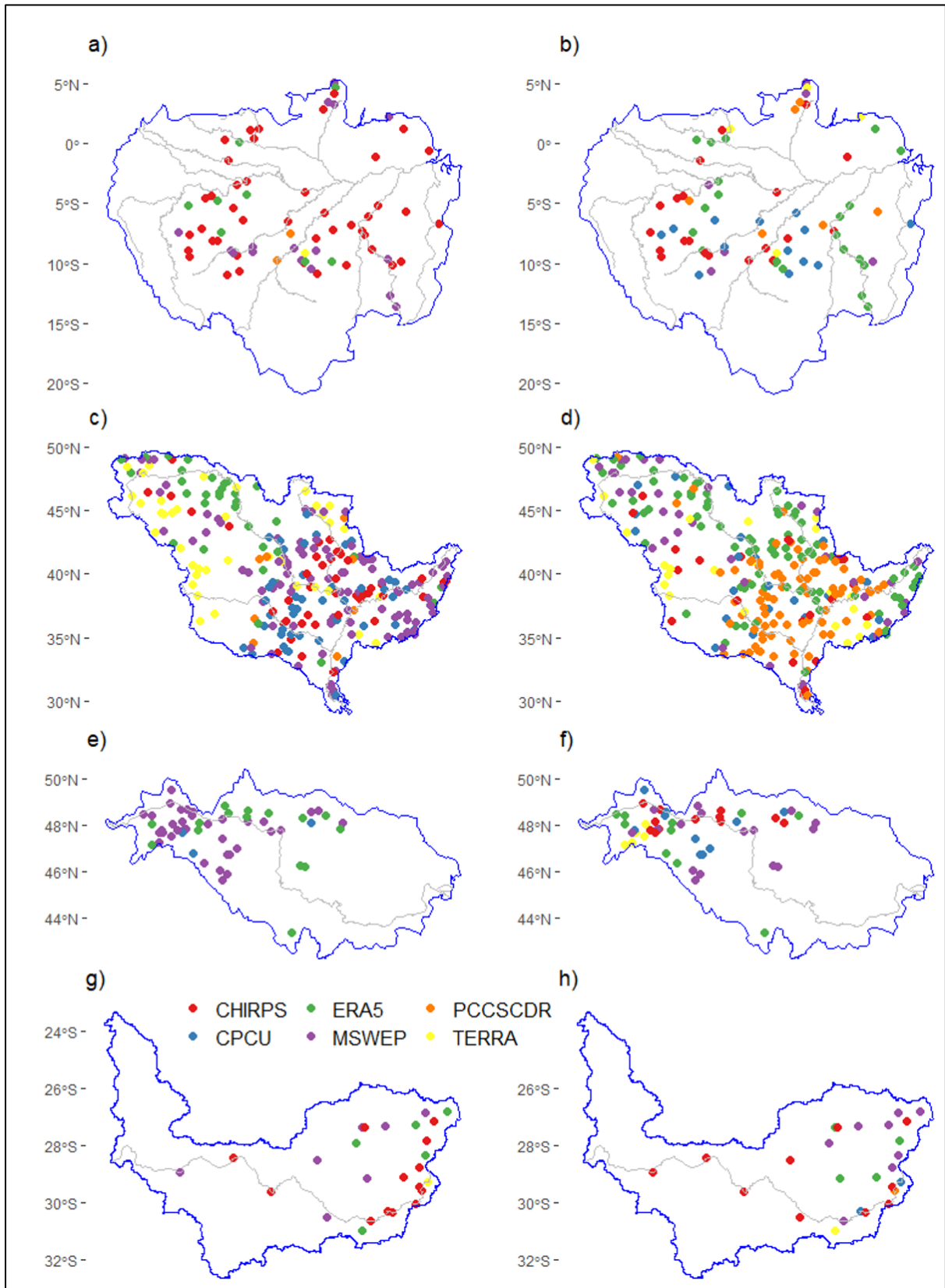


326

327 **Figure 5: Monthly KGE values between observed and modelled streamflow based on a) ERA5, b) CHIRPS, c) MSWEP,**
 328 **d) TERRA, e) CPCU and f) PERCCDR precipitation datasets. KGE values below -0.41 indicate model performance**
 329 **that is worse than using the observed discharge mean as a predictor. The inset histograms show the frequency**
 330 **distribution (y-axis) of the monthly KGE (x-axis). KGE values lower than -1 are highlighted in orange, with the red**
 331 **vertical line indicating the median value.**

332 The spatial representation of the six precipitation datasets in the Amazon, Mississippi, Danube, and Orange River
 333 basins is summarised in Figure 6, highlighting the individual datasets exhibiting the highest CC and KGE values
 334 at each hydrological station. In the Amazon basin, ERA5 (31%) and CHIRPS (29%) emerge as the top performers,
 335 while PERCCDR (8%) and TERRA (5%) rank lower among the precipitation datasets. In the Mississippi basin,
 336 MSWEP leads with higher CC in 37% of stations, and ERA5 holds the top products with higher KGE in 31% of
 337 the stations. Notably, PCCSCDR displays higher KGE values than MSWEP, TERRA, CHIRPS, and CPCU in
 338 30% of Mississippi stations. Across the Danube basin, MSWEP outperforms the other products with a higher CC
 339 in 66% of stations and KGE in 30% of the stations, while TERRA and CPCU are the least performing products.
 340 Furthermore, CHIRPS, in 52% of stations based on CC and 37% based on KGE, outperformed other datasets in

341 the Orange River basin. In Orange, MSWEP ranks second with higher KGE and CC in about 27% of stations,
342 while TERRA and PCCSCDR are the least performing datasets.



343

344 **Figure 6: Performance of precipitation datasets (ERA5, CHIRPS, MSWEP, TERRA, CPCU, and PERCCDR) at**
 345 **discharge stations in a) Amazon, c) Mississippi, e) Danube, and g) Orange river basins based on their monthly CC.**
 346 **Performance of the datasets based on KGE for the Amazon, Mississippi, Danube, and Orange River Basins is illustrated**
 347 **in figures b, d, f, and h, respectively.**

348 Table 2 summarises the monthly KGE between observed and modelled streamflow, based on the six precipitation
 349 datasets, for selected locations in basins of Africa (Niger, Lokoja), Asia (Mekong, Khong-Chiam), South America
 350 (Amazon, Missao-Icana), North America (Mississippi, Savannah), Australia (North East Coast, Mirani-Weir),
 351 and Europe (Danube, Dunaalmas). The basins were chosen to represent a good range of climatic regions and
 352 drainage areas where there was availability of a long time series of observed data (Figure S5). In Niger, the
 353 observed monthly flow and variability at Lokoja station are very well reproduced by CHIRPS and TERRA with
 354 a CC of 0.88 and 0.85, respectively (Figure S5a). Even though CPCU showed a lower CC (0.64) at Lokoja, it
 355 showed a higher KGE (0.62) and lower Pbias (0.4%) compared to the other products. At Lokoja, PERCCDR is
 356 the least well-performing dataset with the highest RMSE and Pbias and lowest KGE. The monthly variability at
 357 the Khong-Chiam station is reproduced by all the precipitation products with a CC of greater than 0.91, with
 358 MSWEP and TERRA showing the lowest bias and RMSE. ERA5 and CHIRPS performed well at station Missao-
 359 Icana in the Amazon with a CC of 0.9 and RMSE of about 610 m3/s. For stations Savannah, Mirani-Weir, and
 360 Dunaalmas, MSWEP is the best product with higher CC (> 0.72) and KGE (> 0.62) and lower Pbias and RMSE
 361 (Figure S5d - S5f).

362 Table 2. KGE of monthly predictions for selected stations in basins of Africa (Niger), Asia (Mekong), South
 363 America (Amazon), North America (Mississippi), Australia (North East Coast), and Europe (Danube).

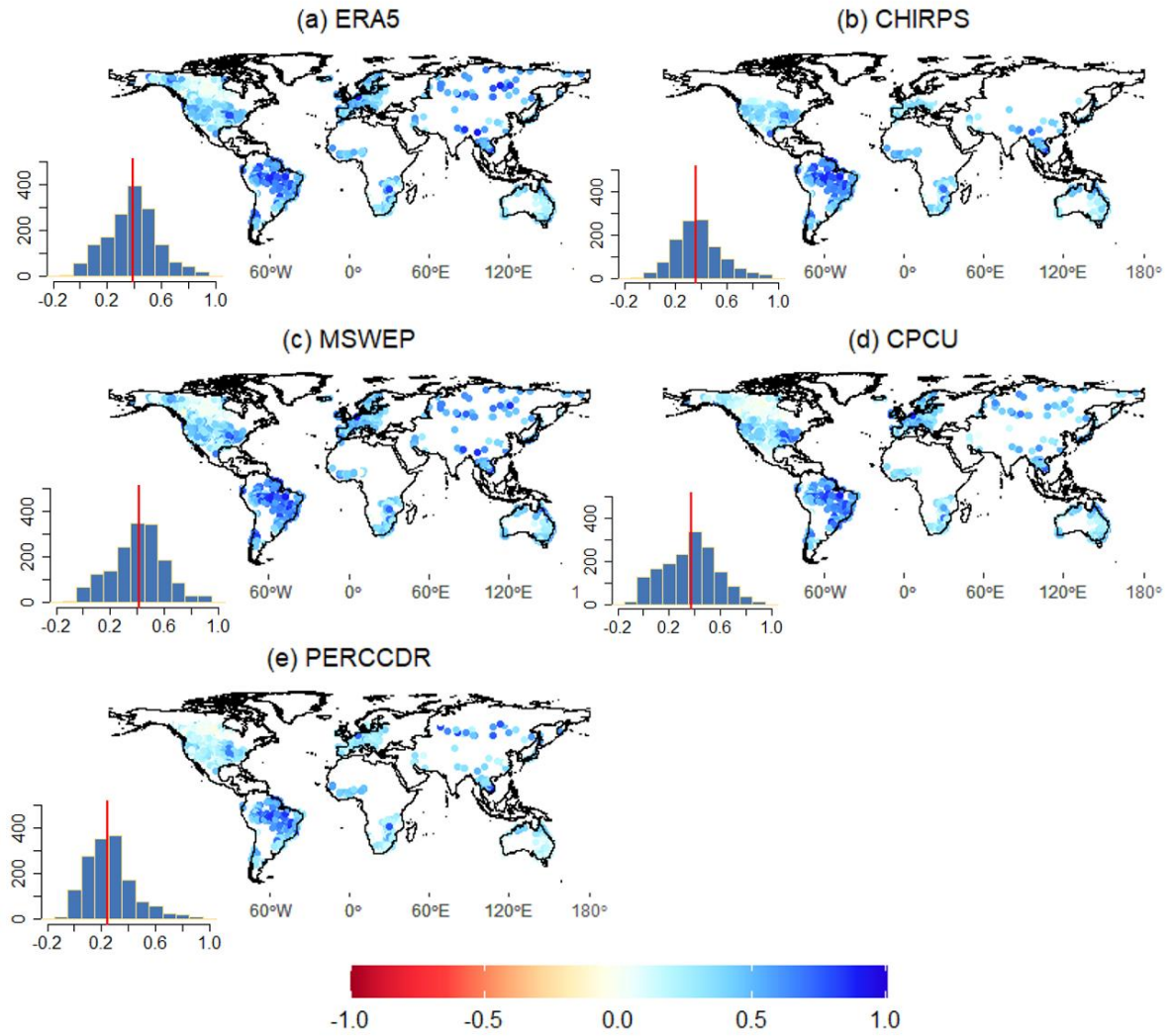
Basin	Stations name	Longitude	Latitude	Catchment area (km ²)	ERA5	CHIRPS	MSWEP	TERRA	CPCU	PERCCDR
Niger	Lokoja	6.8	7.8	1670000	0.21	-0.1	0.60	0.34	0.62	-0.99
Mekong	Khong Chiam	105.5	15.3	419000	0.13	0.56	0.70	0.91	0.70	-0.04
Amazon	Missao Icana	-67.6	1.1	22282	0.71	0.78	0.73	0.72	0.61	0.65
Mississippi	Savannah	-88.3	35.2	85833	0.59	0.65	0.67	0.66	0.53	0.66
North East Coast	Mirani-Weir	148.8	-21.2	1211	-0.1	0.38	0.62	0.44	0.46	-0.05
Danube	Dunaalmas	18.3	47.7	171720	0.34	0.73	0.78	0.52	0.71	-0.49

364

365

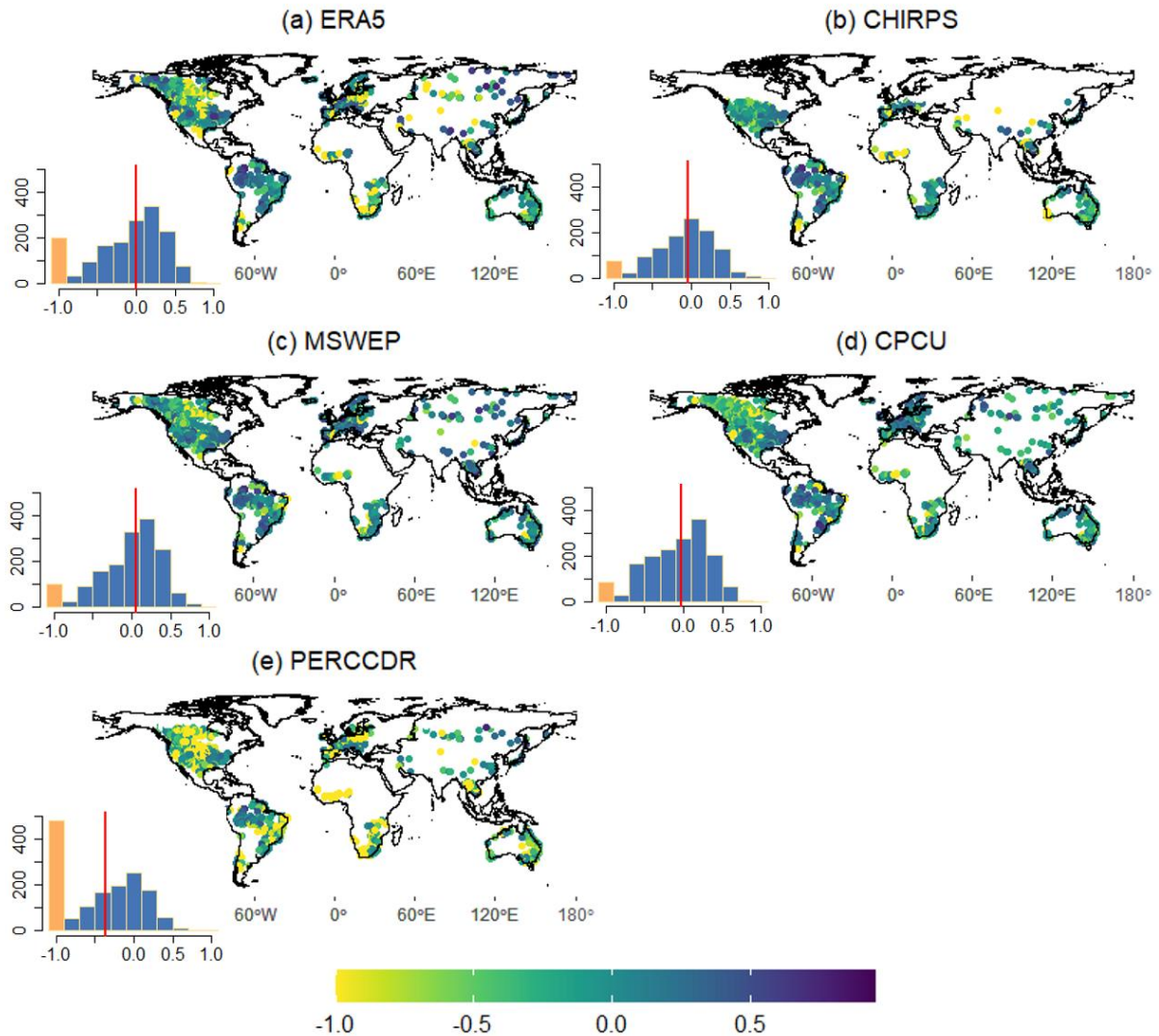
366 **3.3. Performance of the precipitation datasets for daily and daily extreme discharge predictions**

367 Based on the daily evaluation, MSWEP followed by ERA5 show a higher CC in more than 50% of the stations
368 with median values of 0.41 and 0.39, respectively (Figure 7). ERA5 and MSWEP performed well in 31% and
369 31% of the stations with high KGE values (Figure 8). Similar to the monthly evaluation, PERCCDR shows poorer
370 performance (lower CC and KGE, higher biases and errors) in almost 95% of the stations. Even though ERA5
371 showed a higher CC and KGE in 30% of the stations it shows a higher NRMSE (up to 250%) and Pbias (up to
372 100%) in 20% and 30% of the stations (Figures S6 and S7). Overall, MSWEP and CHIRPS showed lower NRMSE
373 and Pbias compared to the other products. The CC and KGE of all the products (except CHIRPS) are lower in
374 North America compared to stations in South America, Europe, and Australia. The spatial representation of
375 precipitation dataset performance, highlighting the individual datasets exhibiting the highest daily CC and KGE
376 values at each observation point, is provided in Figure S9. Additionally, Figure S10 depicts the spatial
377 representation of each precipitation dataset for the Amazon, Mississippi, Danube, and Orange River Basins. In
378 Mississippi, ERA5 exhibited the highest KGE and CC values, followed by MSWEP and CPCU (Figure S10). In
379 the Amazon, ERA5 and CHIRPS displayed the highest KGE and CC values compared to the other datasets. For
380 the Danube, CPCU followed by MSWEP emerged as the best precipitation product relative to ERA5, PCCSCDR,
381 and CHIRPS. In the Orange River Basin, MSWEP based on CC and CHIRPS based on KGE were the top-
382 performing products, while PCCSCDR performed the least.



383

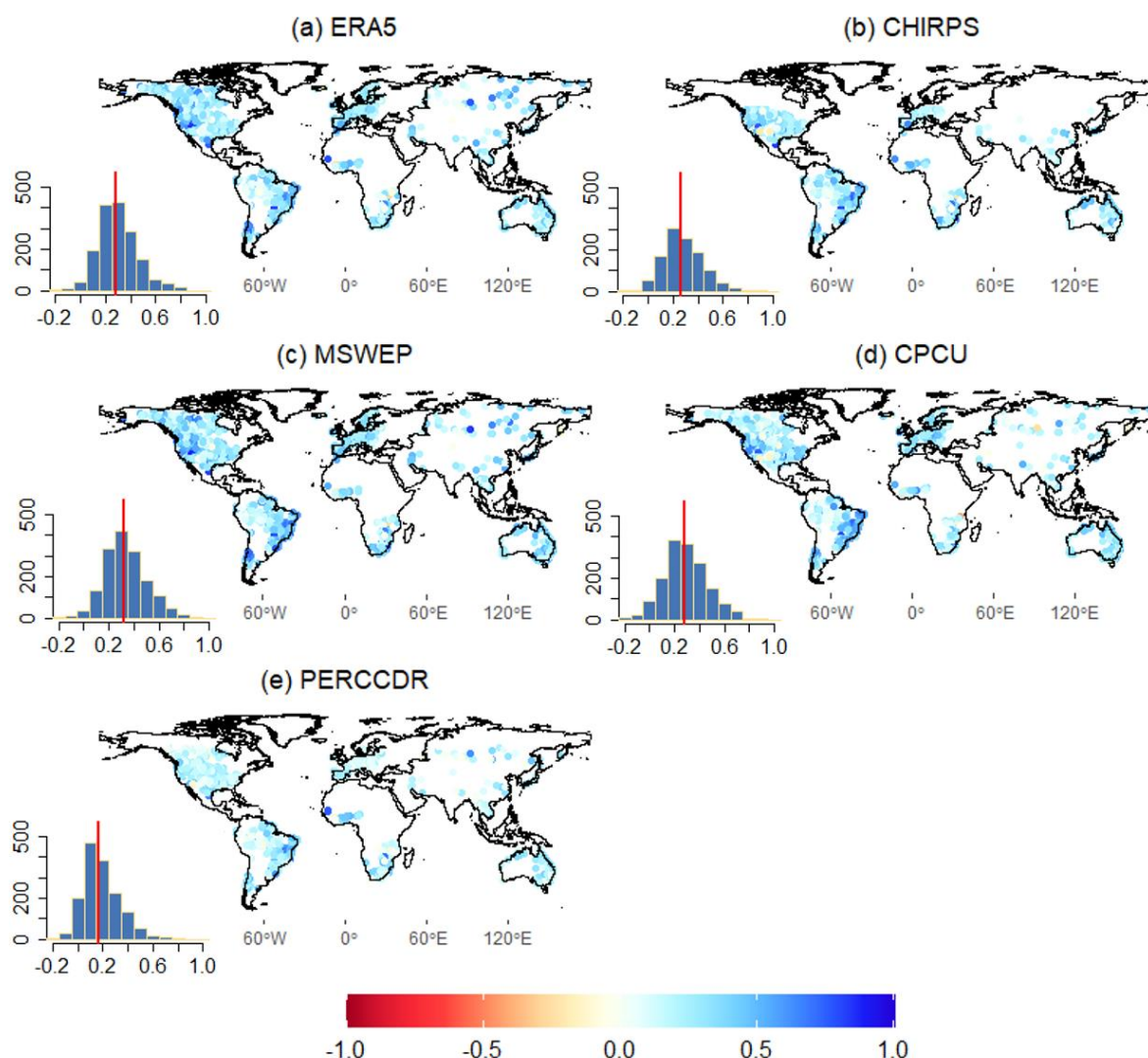
384 **Figure 7: Correlation (CC) between daily observed and modelled streamflow data using a) ERA5, b) CHIRPS, c)**
 385 **MSWEP, d) CPCU and e) PERCCDR precipitation datasets. The inset histograms show the frequency distribution (y-**
 386 **axis) of the daily CC (x-axis), with the red vertical line indicating the median value.**



387

388 **Figure 8: Daily KGE values between observed and modelled streamflow based on a) ERA5, b) CHIRPS, c) MSWEP,**
 389 **d) CPCU, and e) PERCCDR precipitation datasets. KGE values below -0.41 indicate bad model performance than**
 390 **using observed discharge mean as a predictor. The inset histograms show the frequency distribution (y-axis) of the**
 391 **daily KGE (y-axis). KGE values lower than -1 are highlighted in orange, with the red vertical line indicating the median**
 392 **value.**

393 The performance of the daily precipitation products is also assessed for daily extremes in terms of the Q10 and
 394 Q90 values. Based on the CC, MSWEP is the best-performing dataset for Q10 (Figure 9) and Q90 (Figure S8).
 395 For Q10, MSWEP and CPCU exhibited a higher CC than other datasets at 38% and 32% of the stations,
 396 respectively. Similarly, for Q90, MSWEP and ERA demonstrated a higher CC compared to other datasets at 35%
 397 and 30% of the stations. The median CC for Q10 (Q90) is 0.32 (0.41), 0.28 (0.36), 0.27 (0.35), 0.26 (0.38), and
 398 0.16 (0.23) for MSWEP, CPCU, CHIRPS, ERA5, CHIRPS, and PERCCDR, respectively. Similar to the annual,
 399 monthly and daily evaluations, PERCCDR showed poor performance for the two extremes (Q90 and Q10).
 400 Overall, the performance of the datasets is lower for extremes compared to the annual, monthly and daily scales.



401

402 **Figure 9: Correlation (CC) between observed and modelled daily extremes (Q10, high flow) streamflow data a) ERA5,**
 403 **b) CHIRPS, c) MSWEP, d) CPCU and e) PERCCDR precipitation datasets. The inset histograms show the frequency**
 404 **distribution (y-axis) of the daily Q10 CC (x-axis), with the red vertical line indicating the median value.**

405 **4. Discussion and Conclusion**

406 Based on the evaluation at annual, monthly and daily time scales and analysis of daily extremes, no single
 407 precipitation dataset consistently exhibits high accuracy across all geographical regions, nor is one consistently
 408 better than the other datasets. This finding is in line with previous studies (Beck et al., 2017a; Dembélé et al.,
 409 2020). A similar pattern of varied performance (e.g., lower in Africa and the central United States and better in
 410 Europe) by different global hydrological models and precipitation datasets has been presented (Beck et al., 2017a;
 411 Lin et al., 2019; Harrigan et al., 2020). In addition to the uncertainty in the precipitation datasets, the poorer
 412 performance in some regions presented in this and previous studies (Beck et al., 2017a; Lin et al., 2019; Harrigan
 413 et al., 2020) can be due to the lack of representation in the hydrological models of anthropogenic influences, such
 414 as for agriculture, irrigation, water supply, and energy production.

415 Comparably, MSWEP and ERA5 consistently exhibited higher CC and KGE values at over 50% of the stations
416 across annual, monthly, and daily time scales. According to Gu et al. (2023), satellite- and reanalysis-based
417 precipitation datasets, such as MSWEP and ERA5, can provide satisfactory performance for simulating discharge
418 globally. The higher performance of MSWEP indicates the advantage of incorporating a large number of daily
419 observations from field-based meteorological stations, in addition to a large set of satellite and reanalysis datasets
420 (Beck et al., 2017a, 2019a). Other studies have also shown the good performance of MSWEP for hydrological
421 modelling in different parts of the world (Beck et al., 2017a; Lakew, 2020; Li et al., 2022a; Reis et al., 2022; Gu
422 et al., 2023; López López et al., 2017; Satgé et al., 2019; Ibrahim et al., 2022). For example, Satgé et al. (2019)
423 evaluated 12 satellite-based precipitation estimates such as MSWEP, CHIRPS and PERSIANN-CDR in South
424 America (Lake Titicaca region) and found MSWEP was the best precipitation dataset for realistic simulation of
425 river discharge. MSWEP was also found to be the most reliable precipitation dataset compared to multiple datasets
426 such as CHIRPS and CMORPH for hydrological and climate studies in basins of Eastern China (Shaowei et al.,
427 2022; Wu et al., 2018).

428 Even though ERA5 showed a higher KGE and CC than MSWEP, CHIRPS and TERRA in about 32% of the
429 stations it showed a higher error and biases. Previous studies have revealed bias and errors in ERA5 precipitation
430 (Lavers et al., 2021; Bechtold et al., 2020; AL-Falahi et al., 2020; Jiang et al., 2023; Lavers et al., 2022), which
431 leads to propagated errors and bias in hydrological modelling outputs. Harrigan et al. (2020) also reported large
432 biases in ERA5-driven hydrological simulations in the Central United States, South America (e.g., Brazil), and
433 Africa. According to Lavers et al. (2022), ERA5 precipitation is more reliable in extratropical areas compared to
434 tropical areas. Despite CPCU being a gauge-based precipitation dataset, it did not show as good performance as
435 MSWEP and ERA5 on annual, monthly, and daily timescales. In addition to the lower KGE and CC, CPCU
436 showed higher bias and error, particularly on annual and monthly time scales. The bias and errors in CPCU can
437 be due to the coarse resolution (0.5°) and the limited number of stations used to develop the datasets, particularly
438 in Africa and South America. According to Beck et al. (2017a), CPCU can be used in large river basins with dense
439 meteorological stations but can be disadvantageous in Africa and South America. This highlights the need to
440 expand and maintain the meteorological stations in these regions, but also the need to draw from satellite and
441 model data sources. The PERSIANN-CDR is the least-performing product with lower KGE and higher errors and
442 biases, which has been highlighted elsewhere in terms of its inability to represent precipitation extremes (Miao et
443 al., 2015; Solakian et al., 2020).

444 The precipitation datasets show limited skill overall in reproducing daily extremes (high and low flows), relative
445 to the annual and monthly time scales. MSWEP and CPCU have shown a high CC in about 38% of the stations.
446 This is consistent with the findings of Tang et al., (2019) for the Mekong River Basin. CHIRPS and PERSIANN-
447 CDR are the least skilful in capturing extremes with a very low CC and large positive and negative biases (Araujo
448 Palharini et al., 2021). For instance, numerous precipitation products have been observed to both underestimate
449 and overestimate low and high precipitation values in Brazil (Palharini et al., 2020), consequently resulting in
450 corresponding underestimations and overestimations of low and high streamflows. In general, several studies have
451 concluded that precipitation datasets exhibit a substantial disparity in daily extreme precipitation events (e.g.,
452 Araujo Palharini et al., 2021; Jiang et al., 2019; Huang et al., 2022), which can be attributed to factors such as
453 inaccuracies in satellite sensors, retrieval algorithms, temporal sampling, and satellite-observation merging and

454 bias correction procedures used, particularly in gauge-limited regions (Miao et al., 2015; El Kenawy et al., 2015;
455 Shen et al., 2010; Jiang et al., 2019). In addition to the uncertainty of the precipitation datasets, the limited
456 availability of hydrological observations limits the ability to assess these datasets globally, especially for extreme
457 flood and drought events (Brunner et al., 2021).

458 While our study evaluates six global precipitation datasets for hydrological modelling using WBMsed, which
459 show an R^2 of 0.99 in 30-year average prediction against USGS gauge data and global river datasets (Cohen et
460 al., 2022), it is important to acknowledge uncertainties and limitations in both the precipitation data and model
461 parameters. Uncertainties in input data, such as those derived from satellite-based precipitation datasets, including
462 retrieval errors, can propagate through the hydrological model, potentially affecting the accuracy of simulated
463 discharge. Additionally, globally calibrated model parameters may introduce further uncertainty, particularly in
464 regions with limited observational data coverage. Due to the limited availability of observed discharge in Africa
465 and Asia, the evaluation predominantly focuses on North and South America and Europe. Hence, further
466 evaluation in Africa and Asia could be essential to enhance the robustness of global hydrological models.

467 Overall, the evaluation presented in this paper underlines the importance of selecting high-quality precipitation
468 datasets to drive hydrological models. Since no single precipitation dataset was found to be adequately accurate
469 everywhere, this study can help identify the best precipitation products for any basin or region under consideration.
470 Based on our results, MSWEP is the best overall choice but there are regions where ERA5, CHIRPS and CPCU
471 were better overall. All the precipitation datasets, particularly ERA5 and PERCCDR, require bias correction
472 before being used to drive hydrological models in regions like North America, Asia, Africa, and Australia. For
473 data-scarce regions such as Africa and Asia, it is difficult to recommend a precipitation dataset due to the limited
474 number of hydrological stations used in this study. Finally, improving the precipitation datasets by adding more
475 ground observations, for example, and by better representing anthropogenic drivers in hydrological models has
476 the potential of considerably improving global and regional hydrological predictions.

477 **Data availability**

478 The selected precipitation datasets used in this study are openly accessible to the public. ERA5 is freely available
479 from the Copernicus Climate Data Store (CDS; <https://cds.climate.copernicus.eu/cdsapp#!/dataset/reanalysis-era5-land?tab=overview>). CHIRPS can be obtained from the Climate Hazards Group (CHG; <https://www.chc.ucsb.edu/data/chirps/>). Access to the MSWEP precipitation dataset is provided through the
481 GloH2O website (<https://www.gloh2o.org/mswep/>). TERRA is accessible from the Climatology Lab website
482 (<https://www.climatologylab.org/>). CPCU is publicly available through the NOAA Physical Sciences Laboratory
483 (PSL; https://downloads.psl.noaa.gov/Datasets/cpc_global_precip/), and PERCCDR can be freely accessed
484 through the Center for Hydrometeorology and Remote Sensing (CHRS; <https://chrsdata.eng.uci.edu/>).

486 **Author contribution**

487 SG, JL, and SJD: conceptualization. SG: methodology and formal analysis, writing – original draft preparation.
488 JL, SJD, and LS: resources. SC: software and data curation. MW, GB, and RB: investigation, writing – review &
489 editing. PD, HG, and EV: data curation and visualization. YL, RH, LH, SM, and JN: methodology, visualization,
490 investigation, writing – review & editing. PA, HC, AN, AT, and JS: formal analysis, resources, writing – review
491 & editing. DP, SJD, and SED: supervision and project administration.

492 **Competing interests**

493 We declare that Louise Slater is a topical editor of Hydrology and Earth System Sciences (HESS).

494 **Acknowledgements**

495 This work is part of the Evolution of Global Flood Hazard and Risk (EVOFLOOD) project [NE/S015817/1]
496 supported by the Natural Environment Research Council (NERC), the UK Foreign, Commonwealth and
497 Development Office (FCDO) for the benefit of developing countries (Programme Code 201880) and the UK's
498 Natural Environment Research Council (NERC; NE/S017380/1).

499

500

501

502

503

504

505

506

507

508

509

510

511 Reference

512 Abatzoglou, J. T., Dobrowski, S. Z., Parks, S. A., and Hegewisch, K. C.: TerraClimate, a high-resolution global
513 dataset of monthly climate and climatic water balance from 1958–2015, *Sci Data*, 5, 170191,
514 <https://doi.org/10.1038/sdata.2017.191>, 2018.

515 Acharya, S. C., Nathan, R., Wang, Q. J., Su, C.-H., and Eizenberg, N.: An evaluation of daily precipitation from
516 a regional atmospheric reanalysis over Australia, *Hydrology and Earth System Sciences*, 23, 3387–3403,
517 <https://doi.org/10.5194/hess-23-3387-2019>, 2019.

518 Ahmed, K., Shahid, S., Wang, X., Nawaz, N., and Khan, N.: Evaluation of Gridded Precipitation Datasets over
519 Arid Regions of Pakistan, *Water*, 11, 210, <https://doi.org/10.3390/w11020210>, 2019.

520 Alazzy, A. A., Lü, H., Chen, R., Ali, A. B., Zhu, Y., and Su, J.: Evaluation of Satellite Precipitation Products
521 and Their Potential Influence on Hydrological Modeling over the Ganzi River Basin of the Tibetan Plateau,
522 *Advances in Meteorology*, 2017, e3695285, <https://doi.org/10.1155/2017/3695285>, 2017.

523 AL-Falahi, A. H., Saddique, N., Spank, U., Gebrechorkos, S. H., and Bernhofer, C.: Evaluation the Performance
524 of Several Gridded Precipitation Products over the Highland Region of Yemen for Water Resources
525 Management, *Remote Sensing*, 12, 2984, <https://doi.org/10.3390/rs12182984>, 2020.

526 Araujo Palharini, R. S., Vila, D. A., Rodrigues, D. T., Palharini, R. C., Mattos, E. V., and Pedra, G. U.:
527 Assessment of extreme rainfall estimates from satellite-based: Regional analysis, *Remote Sensing Applications:
528 Society and Environment*, 23, 100603, <https://doi.org/10.1016/j.rsase.2021.100603>, 2021.

529 Bárdossy, A., Kilsby, C., Birkinshaw, S., Wang, N., and Anwar, F.: Is Precipitation Responsible for the Most
530 Hydrological Model Uncertainty?, *Frontiers in Water*, 4, 2022.

531 Bechtold, P., R Forbes, I Sandu, S Lang, and M Ahlgrimm: A major moist physics upgrade for the IFS, , 24–32,
532 2020.

533 Beck, H. E., Vergopolan, N., Pan, M., Levizzani, V., Dijk, A. I. J. M. van, Weedon, G. P., Brocca, L.,
534 Pappenberger, F., Huffman, G. J., and Wood, E. F.: Global-scale evaluation of 22 precipitation datasets using
535 gauge observations and hydrological modeling, *Hydrology and Earth System Sciences*, 21, 6201–6217,
536 <https://doi.org/10.5194/hess-21-6201-2017>, 2017a.

537 Beck, H. E., van Dijk, A. I. J. M., Levizzani, V., Schellekens, J., Miralles, D. G., Martens, B., and de Roo, A.:
538 MSWEP: 3-hourly 0.25° global gridded precipitation (1979–2015) by merging gauge, satellite, and reanalysis
539 data, *Hydrology and Earth System Sciences*, 21, 589–615, <https://doi.org/10.5194/hess-21-589-2017>, 2017b.

540 Beck, H. E., Pan, M., Roy, T., Weedon, G. P., Pappenberger, F., van Dijk, A. I. J. M., Huffman, G. J., Adler, R.
541 F., and Wood, E. F.: Daily evaluation of 26 precipitation datasets using Stage-IV gauge-radar data for the
542 CONUS, *Hydrology and Earth System Sciences*, 23, 207–224, <https://doi.org/10.5194/hess-23-207-2019>,
543 2019a.

544 Beck, H. E., Wood, E. F., Pan, M., Fisher, C. K., Miralles, D. G., Dijk, A. I. J. M. van, McVicar, T. R., and
545 Adler, R. F.: MSWEP V2 Global 3-Hourly 0.1° Precipitation: Methodology and Quantitative Assessment,
546 *Bulletin of the American Meteorological Society*, 100, 473–500, <https://doi.org/10.1175/BAMS-D-17-0138.1>,
547 2019b.

548 Brunner, M. I., Slater, L., Tallaksen, L. M., and Clark, M.: Challenges in modeling and predicting floods and
549 droughts: A review, *WIREs Water*, 8, e1520, <https://doi.org/10.1002/wat2.1520>, 2021.

550 Chen, M., Shi, W., Xie, P., Silva, V. B. S., Kousky, V. E., Wayne Higgins, R., and Janowiak, J. E.: Assessing
551 objective techniques for gauge-based analyses of global daily precipitation, *Journal of Geophysical Research:
552 Atmospheres*, 113, <https://doi.org/10.1029/2007JD009132>, 2008.

553 Chen, Y., Hu, D., Duan, X., Zhang, Y., Liu, M., and Shasha, W.: Rainfall-runoff simulation and flood dynamic
554 monitoring based on CHIRPS and MODIS-ET, *International Journal of Remote Sensing*, 41, 4206–4225,
555 <https://doi.org/10.1080/01431161.2020.1714779>, 2020.

556 Cohen, S., Kettner, A. J., Syvitski, J. P. M., and Fekete, B. M.: WBMsed, a distributed global-scale riverine
557 sediment flux model: Model description and validation, *Computers & Geosciences*, 53, 80–93,
558 <https://doi.org/10.1016/j.cageo.2011.08.011>, 2013.

559 Cohen, S., Kettner, A. J., and Syvitski, J. P. M.: Global suspended sediment and water discharge dynamics
560 between 1960 and 2010: Continental trends and intra-basin sensitivity, *Global and Planetary Change*, 115, 44–
561 58, <https://doi.org/10.1016/j.gloplacha.2014.01.011>, 2014.

562 Cohen, S., Syvitski, J., Ashley, T., Lammers, R., Fekete, B., and Li, H.-Y.: Spatial Trends and Drivers of
563 Bedload and Suspended Sediment Fluxes in Global Rivers, *Water Resources Research*, 58, e2021WR031583,
564 <https://doi.org/10.1029/2021WR031583>, 2022.

565 Day, C. A. and Howarth, D. A.: Modeling Climate Change Impacts on the Water Balance of a Medium-Scale
566 Mixed-Forest Watershed, SE USA, *Southeastern Geographer*, 59, 110–129, 2019.

567 Dembélé, M., Schaefli, B., van de Giesen, N., and Mariéthoz, G.: Suitability of 17 gridded rainfall and
568 temperature datasets for large-scale hydrological modelling in West Africa, *Hydrology and Earth System
569 Sciences*, 24, 5379–5406, <https://doi.org/10.5194/hess-24-5379-2020>, 2020.

570 Dunn, F. E., Darby, S. E., Nicholls, R. J., Cohen, S., Zarfl, C., and Fekete, B. M.: Projections of declining
571 fluvial sediment delivery to major deltas worldwide in response to climate change and anthropogenic stress,
572 *Environ. Res. Lett.*, 14, 084034, <https://doi.org/10.1088/1748-9326/ab304e>, 2019.

573 Eini, M. R., Rahmati, A., and Piniewski, M.: Hydrological application and accuracy evaluation of PERSIANN
574 satellite-based precipitation estimates over a humid continental climate catchment, *Journal of Hydrology:*
575 *Regional Studies*, 41, 101109, <https://doi.org/10.1016/j.ejrh.2022.101109>, 2022.

576 El Kenawy, A. M., Lopez-Moreno, J. I., McCabe, M. F., and Vicente-Serrano, S. M.: Evaluation of the TMPA-
577 3B42 precipitation product using a high-density rain gauge network over complex terrain in northeastern Iberia,
578 *Global and Planetary Change*, 133, 188–200, <https://doi.org/10.1016/j.gloplacha.2015.08.013>, 2015.

579 Fallah, A., Rakhshandehroo, G. R., Berg, P., O, S., and Orth, R.: Evaluation of precipitation datasets against
580 local observations in southwestern Iran, *International Journal of Climatology*, 40, 4102–4116,
581 <https://doi.org/10.1002/joc.6445>, 2020.

582 Funk, C., Peterson, P., Landsfeld, M., Pedreros, D., Verdin, J., Shukla, S., Husak, G., Rowland, J., Harrison, L.,
583 Hoell, A., and Michaelsen, J.: The climate hazards infrared precipitation with stations—a new environmental
584 record for monitoring extremes, *Scientific Data*, 2, 150066, <https://doi.org/10.1038/sdata.2015.66>, 2015.

585 Gebrechorkos, S. H., Hülsmann, S., and Bernhofer, C.: Evaluation of multiple climate data sources for
586 managing environmental resources in East Africa, *Hydrology and Earth System Sciences*, 22, 4547–4564,
587 <https://doi.org/10.5194/hess-22-4547-2018>, 2018.

588 Gebrechorkos, S. H., Bernhofer, C., and Hülsmann, S.: Impacts of projected change in climate on water balance
589 in basins of East Africa, *Science of The Total Environment*, <https://doi.org/10.1016/j.scitotenv.2019.05.053>,
590 2019.

591 Gebrechorkos, S. H., Bernhofer, C., and Hülsmann, S.: Climate change impact assessment on the hydrology of a
592 large river basin in Ethiopia using a local-scale climate modelling approach, *Science of The Total Environment*,
593 742, 140504, <https://doi.org/10.1016/j.scitotenv.2020.140504>, 2020.

594 Gebrechorkos, S. H., Leyland, J., Darby, S., and Parsons, D.: High-resolution daily global climate dataset of
595 BCCAQ statistically downscaled CMIP6 models for the EVOFLOOD project. NERC EDS Centre for
596 Environmental Data Analysis, <https://doi.org/10.5285/C107618F1DB34801BB88A1E927B82317>, 2022a.

597 Gebrechorkos, S. H., Pan, M., Beck, H. E., and Sheffield, J.: Performance of State-of-the-Art C3S European
598 Seasonal Climate Forecast Models for Mean and Extreme Precipitation Over Africa, *Water Resources Research*,
599 58, e2021WR031480, <https://doi.org/10.1029/2021WR031480>, 2022b.

600 Gebrechorkos, S. H., Pan, M., Lin, P., Anghileri, D., Forsythe, N., Pritchard, D. M. W., Fowler, H. J., Obuobie,
601 E., Darko, D., and Sheffield, J.: Variability and changes in hydrological drought in the Volta Basin, West
602 Africa, *Journal of Hydrology: Regional Studies*, 42, 101143, <https://doi.org/10.1016/j.ejrh.2022.101143>, 2022c.

603 Gebrechorkos, S. H., Peng, J., Dyer, E., Miralles, D. G., Vicente-Serrano, S. M., Funk, C., Beck, H. E., Asfaw,
604 D. T., Singer, M. B., and Dadson, S. J.: Global High-Resolution Drought Indices for 1981–2022, *Earth
605 System Science Data Discussions*, 1–28, <https://doi.org/10.5194/essd-2023-276>, 2023.

606 Geleta, C. D. and Deressa, T. A.: Evaluation of Climate Hazards Group InfraRed Precipitation Station
607 (CHIRPS) satellite-based rainfall estimates over Finchaa and Neshe Watersheds, Ethiopia, *Engineering Reports*,
608 3, e12338, <https://doi.org/10.1002/eng2.12338>, 2021.

609 GRDC: The Global Runoff Data Centre, 56068 Koblenz, Germany, 2023.

610 Grogan, D. S., Zuidema, S., Prusevich, A., Wollheim, W. M., Glidden, S., and Lammers, R. B.: Water balance
611 model (WBM) v.1.0.0: a scalable gridded global hydrologic model with water-tracking functionality,
612 *Geoscientific Model Development*, 15, 7287–7323, <https://doi.org/10.5194/gmd-15-7287-2022>, 2022.

613 Gu, L., Yin, J., Wang, S., Chen, J., Qin, H., Yan, X., He, S., and Zhao, T.: How well do the multi-satellite and
614 atmospheric reanalysis products perform in hydrological modelling, *Journal of Hydrology*, 617, 128920,
615 <https://doi.org/10.1016/j.jhydrol.2022.128920>, 2023.

616 Guo, B., Zhang, J., Xu, T., Croke, B., Jakeman, A., Song, Y., Yang, Q., Lei, X., and Liao, W.: Applicability
617 Assessment and Uncertainty Analysis of Multi-Precipitation Datasets for the Simulation of Hydrologic Models,
618 *Water*, 10, 1611, <https://doi.org/10.3390/w10111611>, 2018.

619 Gupta, H. V., Kling, H., Yilmaz, K. K., and Martinez, G. F.: Decomposition of the mean squared error and NSE
620 performance criteria: Implications for improving hydrological modelling, *Journal of Hydrology*, 377, 80–91,
621 <https://doi.org/10.1016/j.jhydrol.2009.08.003>, 2009.

622 Hafizi, H. and Sorman, A. A.: Assessment of 13 Gridded Precipitation Datasets for Hydrological Modeling in a
623 Mountainous Basin, *Atmosphere*, 13, 143, <https://doi.org/10.3390/atmos13010143>, 2022.

624 Harrigan, S., Zsoter, E., Alfieri, L., Prudhomme, C., Salamon, P., Wetterhall, F., Barnard, C., Cloke, H., and
625 Pappenberger, F.: GloFAS-ERA5 operational global river discharge reanalysis 1979–present, *Earth System
626 Science Data*, 12, 2043–2060, <https://doi.org/10.5194/essd-12-2043-2020>, 2020.

627 He, Q., Shen, Z., Wan, M., and Li, L.: Precipitable Water Vapor Converted from GNSS-ZTD and ERA5
628 Datasets for the Monitoring of Tropical Cyclones, *IEEE Access*, 8, 87275–87290,
629 <https://doi.org/10.1109/ACCESS.2020.2991094>, 2020.

630 Her, Y., Yoo, S.-H., Cho, J., Hwang, S., Jeong, J., and Seong, C.: Uncertainty in hydrological analysis of
631 climate change: multi-parameter vs. multi-GCM ensemble predictions, *Sci Rep*, 9, 4974,
632 <https://doi.org/10.1038/s41598-019-41334-7>, 2019.

633 Hersbach, H., Bell, B., Berrisford, P., Hirahara, S., Horányi, A., Muñoz-Sabater, J., Nicolas, J., Peubey, C.,
634 Radu, R., Schepers, D., Simmons, A., Soci, C., Abdalla, S., Abellan, X., Balsamo, G., Bechtold, P., Biavati, G.,
635 Bidlot, J., Bonavita, M., De Chiara, G., Dahlgren, P., Dee, D., Diamantakis, M., Dragani, R., Flemming, J.,
636 Forbes, R., Fuentes, M., Geer, A., Haimberger, L., Healy, S., Hogan, R. J., Hólm, E., Janisková, M., Keeley, S.,
637 Laloyaux, P., Lopez, P., Lupu, C., Radnoti, G., de Rosnay, P., Rozum, I., Vamborg, F., Villaume, S., and
638 Thépaut, J.-N.: The ERA5 global reanalysis, *Quarterly Journal of the Royal Meteorological Society*, 146, 1999–
639 2049, <https://doi.org/10.1002/qj.3803>, 2020.

640 Hong, Y., Xuan Do, H., Kessler, J., Fry, L., Read, L., Rafieei Nasab, A., Gronewold, A. D., Mason, L., and
641 Anderson, E. J.: Evaluation of gridded precipitation datasets over international basins and large lakes, *Journal of*
642 *Hydrology*, 607, 127507, <https://doi.org/10.1016/j.jhydrol.2022.127507>, 2022.

643 Hou, D., Charles, M., Luo, Y., Toth, Z., Zhu, Y., Krzysztofowicz, R., Lin, Y., Xie, P., Seo, D.-J., Pena, M., and
644 Cui, B.: Climatology-Calibrated Precipitation Analysis at Fine Scales: Statistical Adjustment of Stage IV toward
645 CPC Gauge-Based Analysis, *Journal of Hydrometeorology*, 15, 2542–2557, <https://doi.org/10.1175/JHM-D-11-0140.1>, 2014.

646 Huang, Z., Zhang, Y., Xu, J., Fang, X., and Ma, Z.: Can satellite precipitation estimates capture the magnitude
647 of extreme rainfall Events?, *Remote Sensing Letters*, 13, 1048–1057,
648 <https://doi.org/10.1080/2150704X.2022.2123258>, 2022.

649 van Huijgevoort, M. H. J., Hazenberg, P., van Lanen, H. a. J., Teuling, A. J., Clark, D. B., Folwell, S., Gosling,
650 S. N., Hanasaki, N., Heinke, J., Koirala, S., Stacke, T., Voss, F., Sheffield, J., and Uijlenhoet, R.: Global
651 Multimodel Analysis of Drought in Runoff for the Second Half of the Twentieth Century, *J. Hydrometeor.*, 14,
652 1535–1552, <https://doi.org/10.1175/JHM-D-12-0186.1>, 2013.

653 Ibrahim, A. H., Molla, D. D., and Lohani, T. K.: Performance evaluation of satellite-based rainfall estimates for
654 hydrological modeling over Bilate river basin, Ethiopia, *World Journal of Engineering*, ahead-of-print,
655 <https://doi.org/10.1108/WJE-03-2022-0106>, 2022.

656 Jiang, Q., Li, W., Wen, J., Fan, Z., Chen, Y., Scaioni, M., and Wang, J.: Evaluation of satellite-based products
657 for extreme rainfall estimations in the eastern coastal areas of China, *Journal of Integrative Environmental*
658 *Sciences*, 16, 191–207, <https://doi.org/10.1080/1943815X.2019.1707233>, 2019.

659 Jiang, S., Wei, L., Ren, L., Zhang, L., Wang, M., and Cui, H.: Evaluation of IMERG, TMPA, ERA5, and CPC
660 precipitation products over mainland China: Spatiotemporal patterns and extremes, *Water Science and*
661 *Engineering*, 16, 45–56, <https://doi.org/10.1016/j.wse.2022.05.001>, 2023.

662 Jiao, D., Xu, N., Yang, F., and Xu, K.: Evaluation of spatial-temporal variation performance of ERA5
663 precipitation data in China, *Sci Rep*, 11, 17956, <https://doi.org/10.1038/s41598-021-97432-y>, 2021.

664 Kidd, C. and Levizzani, V.: Status of satellite precipitation retrievals, *Hydrology and Earth System Sciences*, 15,
665 1109–1116, <https://doi.org/10.5194/hess-15-1109-2011>, 2011.

666 Kidd, C., Becker, A., Huffman, G. J., Muller, C. L., Joe, P., Skofronick-Jackson, G., and Kirschbaum, D. B.: So,
667 How Much of the Earth’s Surface Is Covered by Rain Gauges?, *Bulletin of the American Meteorological*
668 *Society*, 98, 69–78, <https://doi.org/10.1175/BAMS-D-14-00283.1>, 2017.

669 Knoben, W. J. M., Freer, J. E., and Woods, R. A.: Technical note: Inherent benchmark or not? Comparing
670 Nash–Sutcliffe and Kling–Gupta efficiency scores, *Hydrology and Earth System Sciences*, 23, 4323–4331,
671 <https://doi.org/10.5194/hess-23-4323-2019>, 2019.

672 Laiti, L., Mallucci, S., Piccolroaz, S., Bellin, A., Zardi, D., Fiori, A., Nikulin, G., and Majone, B.: Testing the
673 Hydrological Coherence of High-Resolution Gridded Precipitation and Temperature Data Sets, *Water Resources*
674 *Research*, 54, 1999–2016, <https://doi.org/10.1002/2017WR021633>, 2018.

675 Lakew, H. B.: Investigating the effectiveness of bias correction and merging MSWEP with gauged rainfall for
676 the hydrological simulation of the upper Blue Nile basin, *Journal of Hydrology: Regional Studies*, 32, 100741,
677 <https://doi.org/10.1016/j.ejrh.2020.100741>, 2020.

678 Lavers, D. A., Harrigan, S., and Prudhomme, C.: Precipitation Biases in the ECMWF Integrated Forecasting
679 System, *Journal of Hydrometeorology*, 22, 1187–1198, <https://doi.org/10.1175/JHM-D-20-0308.1>, 2021.

680 Lavers, D. A., Simmons, A., Vamborg, F., and Rodwell, M. J.: An evaluation of ERA5 precipitation for climate
681 monitoring, *Quarterly Journal of the Royal Meteorological Society*, 148, 3152–3165,
682 <https://doi.org/10.1002/qj.4351>, 2022.

683 Lehner, B., Verdin, K. L., and Jarvis, A.: New global hydrography derived from spaceborne elevation data, *Eos*,
684 *Transactions, American Geophysical Union*, 89, 2, <https://doi.org/10.1029/2008EO100001>, 2008.

685 Lehner, B., Liermann, C. R., Revenga, C., Vörösmarty, C., Fekete, B., Crouzet, P., Döll, P., Endean, M.,
686 Frenken, K., Magome, J., Nilsson, C., Robertson, J. C., Rödel, R., Sindorf, N., and Wisser, D.: High-resolution
687 mapping of the world’s reservoirs and dams for sustainable river-flow management, *Frontiers in Ecology and*
688 *the Environment*, 9, 494–502, <https://doi.org/10.1890/100125>, 2011.

689 Li, L., Wang, Y., Wang, L., Hu, Q., Zhu, Z., Li, L., and Li, C.: Spatio-temporal accuracy evaluation of MSWEP
690 daily precipitation over the Huaihe River Basin, China: A comparison study with representative satellite- and
691 reanalysis-based products, *J. Geogr. Sci.*, 32, 2271–2290, <https://doi.org/10.1007/s11442-022-2047-9>, 2022a.

693 Li, M., Lv, X., Zhu, L., Uchenna Ochege, F., and Guo, H.: Evaluation and Application of MSWEP in Drought
694 Monitoring in Central Asia, *Atmosphere*, 13, 1053, <https://doi.org/10.3390/atmos13071053>, 2022b.

695 Lin, P., Pan, M., Beck, H. E., Yang, Y., Yamazaki, D., Frasson, R., David, C. H., Durand, M., Pavelsky, T. M.,
696 Allen, G. H., Gleason, C. J., and Wood, E. F.: Global Reconstruction of Naturalized River Flows at 2.94 Million
697 Reaches, *Water Resources Research*, 55, 6499–6516, <https://doi.org/10.1029/2019WR025287>, 2019.

698 López López, P., Sutanudjaja, E. H., Schellekens, J., Sterk, G., and Bierkens, M. F. P.: Calibration of a large-
699 scale hydrological model using satellite-based soil moisture and evapotranspiration products, *Hydrology and
700 Earth System Sciences*, 21, 3125–3144, <https://doi.org/10.5194/hess-21-3125-2017>, 2017.

701 Luo, X., Wu, W., He, D., Li, Y., and Ji, X.: Hydrological Simulation Using TRMM and CHIRPS Precipitation
702 Estimates in the Lower Lancang-Mekong River Basin, *Chin. Geogr. Sci.*, 29, 13–25,
703 <https://doi.org/10.1007/s11769-019-1014-6>, 2019.

704 Maggioni, V. and Massari, C.: On the performance of satellite precipitation products in riverine flood modeling:
705 A review, *Journal of Hydrology*, 558, 214–224, <https://doi.org/10.1016/j.jhydrol.2018.01.039>, 2018.

706 Mazzoleni, M., Brandimarte, L., and Amaranto, A.: Evaluating precipitation datasets for large-scale distributed
707 hydrological modelling, *Journal of Hydrology*, 578, 124076, <https://doi.org/10.1016/j.jhydrol.2019.124076>,
708 2019.

709 Mehran, A. and AghaKouchak, A.: Capabilities of satellite precipitation datasets to estimate heavy precipitation
710 rates at different temporal accumulations, *Hydrological Processes*, 28, 2262–2270,
711 <https://doi.org/10.1002/hyp.9779>, 2014.

712 Menne, M. J., Durre, I., Vose, R. S., Gleason, B. E., and Houston, T. G.: An Overview of the Global Historical
713 Climatology Network-Daily Database, *Journal of Atmospheric and Oceanic Technology*, 29, 897–910,
714 <https://doi.org/10.1175/JTECH-D-11-00103.1>, 2012.

715 Mianabadi, A., Salari, K., and Pourmohamad, Y.: Drought monitoring using the long-term CHIRPS
716 precipitation over Southeastern Iran, *Appl Water Sci*, 12, 183, <https://doi.org/10.1007/s13201-022-01705-4>,
717 2022.

718 Miao, C., Ashouri, H., Hsu, K.-L., Sorooshian, S., and Duan, Q.: Evaluation of the PERSIANN-CDR Daily
719 Rainfall Estimates in Capturing the Behavior of Extreme Precipitation Events over China, *Journal of
720 Hydrometeorology*, 16, 1387–1396, <https://doi.org/10.1175/JHM-D-14-0174.1>, 2015.

721 Miao, Q., Pan, B., Wang, H., Hsu, K., and Sorooshian, S.: Improving Monsoon Precipitation Prediction Using
722 Combined Convolutional and Long Short Term Memory Neural Network, *Water*, 11, 977,
723 <https://doi.org/10.3390/w11050977>, 2019.

724 Michaelides, S., Levizzani, V., Anagnostou, E., Bauer, P., Kasparis, T., and Lane, J. E.: Precipitation:
725 Measurement, remote sensing, climatology and modeling, *Atmospheric Research*, 94, 512–533,
726 <https://doi.org/10.1016/j.atmosres.2009.08.017>, 2009.

727 Moazami, S., Golian, S., Kavianpour, M. R., and Hong, Y.: Comparison of PERSIANN and V7 TRMM Multi-
728 satellite Precipitation Analysis (TMPA) products with rain gauge data over Iran, *International Journal of Remote
729 Sensing*, 34, 8156–8171, <https://doi.org/10.1080/01431161.2013.833360>, 2013.

730 Moragoda, N. and Cohen, S.: Climate-induced trends in global riverine water discharge and suspended sediment
731 dynamics in the 21st century, *Global and Planetary Change*, 191, 103199,
732 <https://doi.org/10.1016/j.gloplacha.2020.103199>, 2020.

733 Nguyen, P., Thorstensen, A., Sorooshian, S., Hsu, K., Aghakouchak, A., Ashouri, H., Tran, H., and Braithwaite,
734 D.: Global Precipitation Trends across Spatial Scales Using Satellite Observations, *Bulletin of the American
735 Meteorological Society*, 99, 689–697, <https://doi.org/10.1175/BAMS-D-17-0065.1>, 2018.

736 Opere, A. O., Waswa, R., and Mutua, F. M.: Assessing the Impacts of Climate Change on Surface Water
737 Resources Using WEAP Model in Narok County, Kenya, *Frontiers in Water*, 3, 2022.

738 Palharini, R. S. A., Vila, D. A., Rodrigues, D. T., Quispe, D. P., Palharini, R. C., de Siqueira, R. A., and de
739 Sousa Afonso, J. M.: Assessment of the Extreme Precipitation by Satellite Estimates over South America,
740 *Remote Sensing*, 12, 2085, <https://doi.org/10.3390/rs12132085>, 2020.

741 Parker, W. S.: Reanalyses and Observations: What’s the Difference?, *Bulletin of the American Meteorological
742 Society*, 97, 1565–1572, <https://doi.org/10.1175/BAMS-D-14-00226.1>, 2016.

743 Peng, J., Dadson, S., Hirpa, F., Dyer, E., Lees, T., Miralles, D. G., Vicente-Serrano, S. M., and Funk, C.: A pan-
744 African high-resolution drought index dataset, *Earth System Science Data*, 12, 753–769,
745 <https://doi.org/10.5194/essd-12-753-2020>, 2020.

746 Raimonet, M., Oudin, L., Thieu, V., Silvestre, M., Vautard, R., Rabouille, C., and Moigne, P. L.: Evaluation of
747 Gridded Meteorological Datasets for Hydrological Modeling, *Journal of Hydrometeorology*, 18, 3027–3041,
748 <https://doi.org/10.1175/JHM-D-17-0018.1>, 2017.

749 Reichle, R. H., Koster, R. D., Lannoy, G. J. M. D., Forman, B. A., Liu, Q., Mahanama, S. P. P., and Touré, A.:
750 Assessment and Enhancement of MERRA Land Surface Hydrology Estimates, *Journal of Climate*, 24, 6322–
751 6338, <https://doi.org/10.1175/JCLI-D-10-05033.1>, 2011.

752 Reis, A. A. dos, Weerts, A., Ramos, M.-H., Wetterhall, F., and Fernandes, W. dos S.: Hydrological data and
753 modeling to combine and validate precipitation datasets relevant to hydrological applications, *Journal of*
754 *Hydrology: Regional Studies*, 44, 101200, <https://doi.org/10.1016/j.ejrh.2022.101200>, 2022.

755 Sadeghi, M., Nguyen, P., Naeini, M. R., Hsu, K., Braithwaite, D., and Sorooshian, S.: PERSIANN-CCS-CDR, a
756 3-hourly 0.04° global precipitation climate data record for heavy precipitation studies, *Sci Data*, 8, 157,
757 <https://doi.org/10.1038/s41597-021-00940-9>, 2021.

758 Salehi, H., Sadeghi, M., Golian, S., Nguyen, P., Murphy, C., and Sorooshian, S.: The Application of
759 PERSIANN Family Datasets for Hydrological Modeling, *Remote Sensing*, 14, 3675,
760 <https://doi.org/10.3390/rs14153675>, 2022.

761 Satgé, F., Ruelland, D., Bonnet, M.-P., Molina, J., and Pillco, R.: Consistency of satellite-based precipitation
762 products in space and over time compared with gauge observations and snow- hydrological modelling in the
763 Lake Titicaca region, *Hydrology and Earth System Sciences*, 23, 595–619, [https://doi.org/10.5194/hess-23-595-](https://doi.org/10.5194/hess-23-595-2019)
764 2019, 2019.

765 Seyyedi, H., Anagnostou, E. N., Beighley, E., and McCollum, J.: Hydrologic evaluation of satellite and
766 reanalysis precipitation datasets over a mid-latitude basin, *Atmospheric Research*, 164–165, 37–48,
767 <https://doi.org/10.1016/j.atmosres.2015.03.019>, 2015.

768 Shaowei, N., Jie, W., Juliang, J., Xiaoyan, X., Yuliang, Z., Fan, S., and Linlin, Z.: Comprehensive evaluation of
769 satellite-derived precipitation products considering spatial distribution difference of daily precipitation over
770 eastern China, *Journal of Hydrology: Regional Studies*, 44, 101242, <https://doi.org/10.1016/j.ejrh.2022.101242>,
771 2022.

772 Sheffield, J., Goteti, G., and Wood, E. F.: Development of a 50-Year High-Resolution Global Dataset of
773 Meteorological Forcings for Land Surface Modeling, *J. Climate*, 19, 3088–3111,
774 <https://doi.org/10.1175/JCLI3790.1>, 2006.

775 Sheffield, J., Wood, E. F., Pan, M., Beck, H., Coccia, G., Serrat-Capdevila, A., and Verbist, K.: Satellite Remote
776 Sensing for Water Resources Management: Potential for Supporting Sustainable Development in Data-Poor
777 Regions, *Water Resources Research*, 54, 9724–9758, <https://doi.org/10.1029/2017WR022437>, 2018.

778 Shen, Y., Xiong, A., Wang, Y., and Xie, P.: Performance of high-resolution satellite precipitation products over
779 China, *Journal of Geophysical Research: Atmospheres*, 115, <https://doi.org/10.1029/2009JD012097>, 2010.

780 Solakian, J., Maggioni, V., and Godrej, A. N.: On the Performance of Satellite-Based Precipitation Products in
781 Simulating Streamflow and Water Quality During Hydrometeorological Extremes, *Frontiers in Environmental*
782 *Science*, 8, 2020.

783 Sun, G., Wei, Y., Wang, G., Shi, R., Chen, H., and Mo, C.: Downscaling Correction and Hydrological
784 Applicability of the Three Latest High-Resolution Satellite Precipitation Products (GPM, GSMAP, and
785 MSWEP) in the Pingtang Catchment, China, *Advances in Meteorology*, 2022, e6507109,
786 <https://doi.org/10.1155/2022/6507109>, 2022.

787 Sun, Q., Miao, C., Duan, Q., Ashouri, H., Sorooshian, S., and Hsu, K.-L.: A Review of Global Precipitation
788 Data Sets: Data Sources, Estimation, and Intercomparisons, *Reviews of Geophysics*, 56, 79–107,
789 <https://doi.org/10.1002/2017RG000574>, 2018.

790 Tang, X., Zhang, J., Gao, C., Ruben, G. B., and Wang, G.: Assessing the Uncertainties of Four Precipitation
791 Products for Swat Modeling in Mekong River Basin, *Remote Sensing*, 11, 304,
792 <https://doi.org/10.3390/rs11030304>, 2019.

793 Ursulak, J. and Coulibaly, P.: Integration of hydrological models with entropy and multi-objective optimization
794 based methods for designing specific needs streamflow monitoring networks, *Journal of Hydrology*, 593,
795 125876, <https://doi.org/10.1016/j.jhydrol.2020.125876>, 2021.

796 Voisin, N., Wood, A. W., and Lettenmaier, D. P.: Evaluation of Precipitation Products for Global Hydrological
797 Prediction, *Journal of Hydrometeorology*, 9, 388–407, <https://doi.org/10.1175/2007JHM938.1>, 2008.

798 Wang, M., Rezaie-Balf, M., Naganna, S. R., and Yaseen, Z. M.: Sourcing CHIRPS precipitation data for
799 streamflow forecasting using intrinsic time-scale decomposition based machine learning models, *Hydrological*
800 *Sciences Journal*, 66, 1437–1456, <https://doi.org/10.1080/02626667.2021.1928138>, 2021.

801 Wang, N., Liu, W., Sun, F., Yao, Z., Wang, H., and Liu, W.: Evaluating satellite-based and reanalysis
802 precipitation datasets with gauge-observed data and hydrological modeling in the Xihe River Basin, China,
803 *Atmospheric Research*, 234, 104746, <https://doi.org/10.1016/j.atmosres.2019.104746>, 2020.

804 Wati, T., Hadi, T. W., Sopaheluwakan, A., and Hutasoit, L. M.: Statistics of the Performance of Gridded
805 Precipitation Datasets in Indonesia, *Advances in Meteorology*, 2022, e7995761,
806 <https://doi.org/10.1155/2022/7995761>, 2022.

807 Wissler, D., Fekete, B. M., Vörösmarty, C. J., and Schumann, A. H.: Reconstructing 20th century global
808 hydrography: a contribution to the Global Terrestrial Network- Hydrology (GTN-H), *Hydrology and Earth*
809 *System Sciences*, 14, 1–24, <https://doi.org/10.5194/hess-14-1-2010>, 2010.

810 Wollheim, W. M., Vörösmarty, C. J., Bouwman, A. F., Green, P., Harrison, J., Linder, E., Peterson, B. J.,
811 Seitzinger, S. P., and Syvitski, J. P. M.: Global N removal by freshwater aquatic systems using a spatially

812 distributed, within-basin approach, *Global Biogeochemical Cycles*, 22, <https://doi.org/10.1029/2007GB002963>,
813 2008.

814 Wu, Z., Xu, Z., Wang, F., He, H., Zhou, J., Wu, X., and Liu, Z.: Hydrologic Evaluation of Multi-Source
815 Satellite Precipitation Products for the Upper Huaihe River Basin, China, *Remote Sensing*, 10, 840,
816 <https://doi.org/10.3390/rs10060840>, 2018.

817 Xiang, Y., Chen, J., Li, L., Peng, T., and Yin, Z.: Evaluation of Eight Global Precipitation Datasets in
818 Hydrological Modeling, *Remote Sensing*, 13, 2831, <https://doi.org/10.3390/rs13142831>, 2021.

819 Zambrano-Bigiarini, M., Nauditt, A., Birkel, C., Verbist, K., and Ribbe, L.: Temporal and spatial evaluation of
820 satellite-based rainfall estimates across the complex topographical and climatic gradients of Chile, *Hydrology*
821 *and Earth System Sciences Discussions*, 1–43, <https://doi.org/10.5194/hess-2016-453>, 2016.

822 Zhu, D., Ilyas, A. M., Wang, G., and Zeng, B.: Long-term hydrological assessment of remote sensing
823 precipitation from multiple sources over the lower Yangtze River basin, China, *Meteorological Applications*, 28,
824 e1991, <https://doi.org/10.1002/met.1991>, 2021.

825 Zhu, H., Li, Y., Huang, Y., Li, Y., Hou, C., and Shi, X.: Evaluation and hydrological application of satellite-
826 based precipitation datasets in driving hydrological models over the Huifa river basin in Northeast China,
827 *Atmospheric Research*, 207, 28–41, <https://doi.org/10.1016/j.atmosres.2018.02.022>, 2018.

828